Improving the Representation of Physical Atmosphere in Air Quality Decision Support Systems Used for Emissions Control Strategy Development

Arastoo Pour Biazar[1], Richard T. McNider[1], Daniel Cohan[2]

Collaborators

A. Kaduwala[3], Z. Zhao[3], S. Tanrikulu[4], B. Dornblaser[5], M. Estes[5], J. Boylan[6], G. Jedlovec[7], J. E. Pleim[8], Pius Lee[9]

1. University of Alabama in Huntsville (UAH)
2. Rice University
3. California Air Resources Board (CARB)
4. Bay Area Air Quality Management District (BAAQMD)
5. Texas Commission on Environmental Quality (TCEQ)
6. Georgia Environmental Protection Division (Georgia-EPD)
7. National Aeronautics and Space Administration (NASA)
8. Environmental Protection Agency (EPA)
9. National Oceanic and Atmospheric Administration (NOAA)

Presented at:

Health and Air Quality Applications Program Review
September 16–17, 2015, Park City, Utah

PROJECT SUMMARY

TOPIC: **Improving the Representation of Physical Atmosphere in Air Quality Decision Support Systems Used for Emissions Control Strategy Development**

POP: 6/24/1/2015 – 6/23/2018 (ROSES2013-A.44)

PI: Arastoo Pour Biazar (University of Alabama – Huntsville)
Co-Is: Dick McNider (UAH), Daniel Cohan (Rice)

Partners: California Air Resources Board (CARB), Bay Area Air Quality Management District (BAAQMD), USEPA, Texas Commission on Environmental Quality (TCEQ), Georgia Environmental Protection Division (GA-EPD), National Oceanic and Atmospheric Administration (NOAA)

NASA Assets: NASA's GOES Product Generation System (skin T, surface insolation and albedo); MODIS products (Skin Temperature, surface insolation and albedo)

Objective: To employ NASA assets and satellite products to improve the air quality management Decision Support Tools (DSTs) used in defining emission control strategies for attainment of air quality standards.

Bay Area Air Quality Management District | California Air Resources Board | Georgia | TCEQ | NASA | NOAA | NSSTC | RICE | The University of Alabama in Huntsville

Overall Objective: To Reduce the Uncertainties in Regulatory Air Quality Simulations Through the Use of NASA Science and Satellite Data Products

In SIP modeling it is imperative to reproduce the observed atmosphere. Model uncertainties translates into uncertainties in emission control strategy which has significant economic consequences.

Physical Atmosphere

Models: WRF, MM5, RAMS
Recreates the physical atmosphere (winds, temperature, precipitation, moisture, turbulence etc) during the design period

Clouds and microphysical processes

Atmospheric dynamics

Boundary layer development

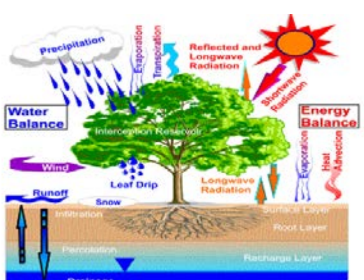

Fluxes of heat and moisture

LSM describing land-atmosphere interactions

Winds, temperature, BL height, Radiation, moisture, surface properties and fluxes, precipitation

Chemical Atmosphere

Models: CMAQ, CAMx
Recreates the chemical atmosphere

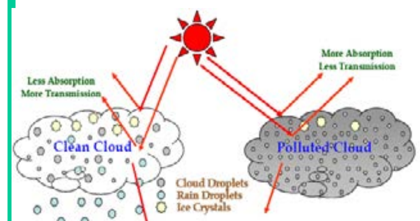

Heterogeneous chemistry, aerosol

Transport and transformation of pollutants

Photochemistry and oxidant formation

Natural and antropogenic emissions, Surface removal




Contribution of This Project in Reducing Simulation Uncertainties

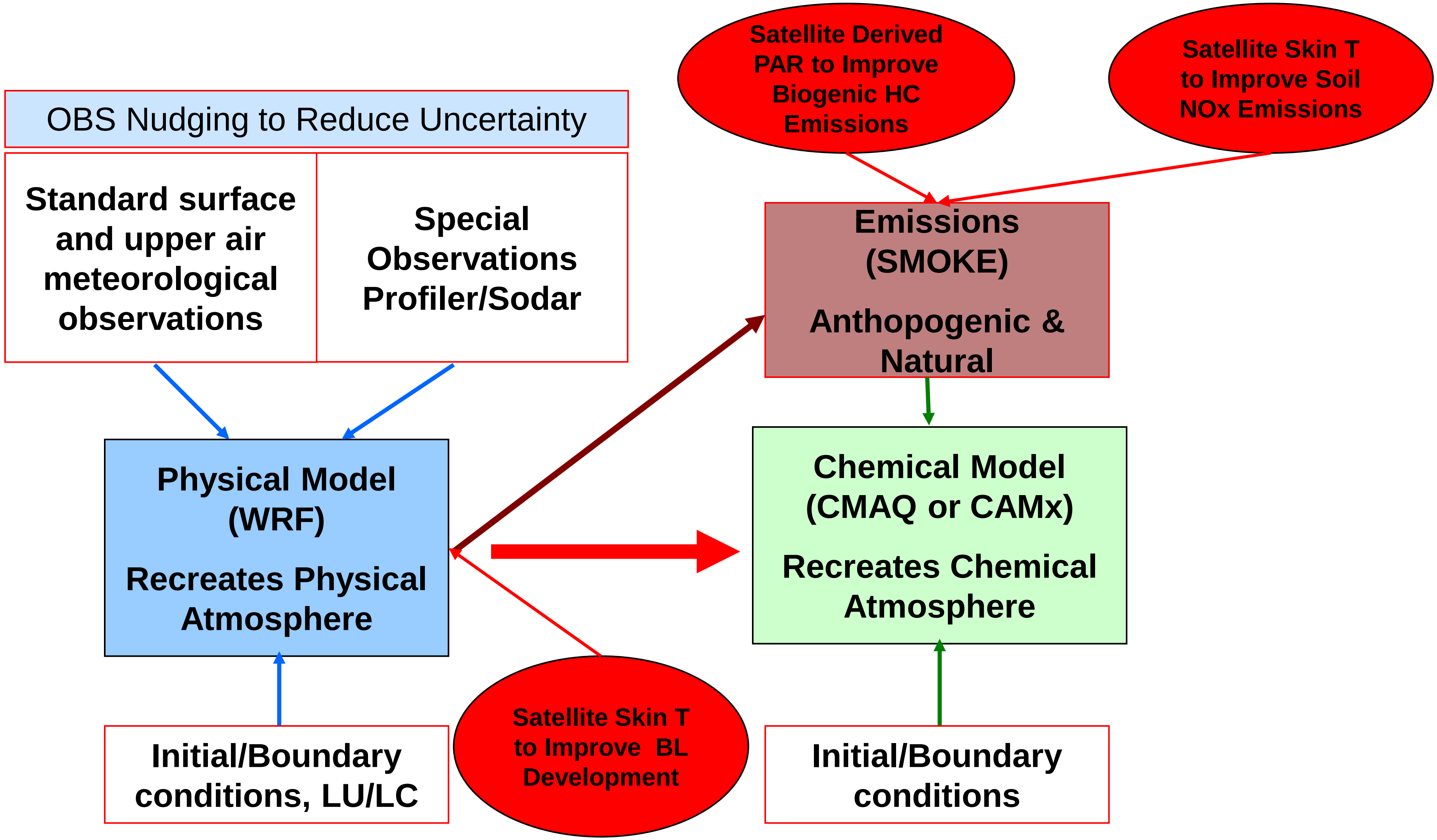

Specific Objectives

In This Project NASA Assets and Satellite Data Will Be Used to Improve the Quality and Accuracy of Retrospective Baseline Simulation in Which Proposed SIP Emission Reductions Are Tested

Improving Emission Estimates in AQ Model

- **Utilization of Satellite Derived Photosynthetically Active Radiation (PAR) to Improve Biogenic Hydrocarbon Emissions:** This activity utilizes NASA's GOES Product Generation System (GPGS) to produce PAR (a new product) for use in AQ models.
- **Improving Soil Nox Emission Estimates:** By including the impact of satellite derived temperature and soil moisture.

Improving Physical Atmosphere

- **Improved Characterization of Surface Energy Budget:** Using satellite derived skin temperature to retrieve soil moisture and correct surface heat fluxes.
- **Improving Boundary Layer Development in the Model:** By improving BL moisture and temperature structure.

- BVOC estimates depend on the amount of radiation reaching the canopy (i.e. Photosynthetically Active Radiation (PAR)) and temperature.
- Large uncertainty is caused by the model insolation estimates that can be corrected by using satellite-based PAR in biogenic emission models (Guenther et al. 2012)

hv

NOx + VOC + *hv* $\rightarrow O_3$

Biogenic Volatile Organic Compounds (BVOC) Emissions

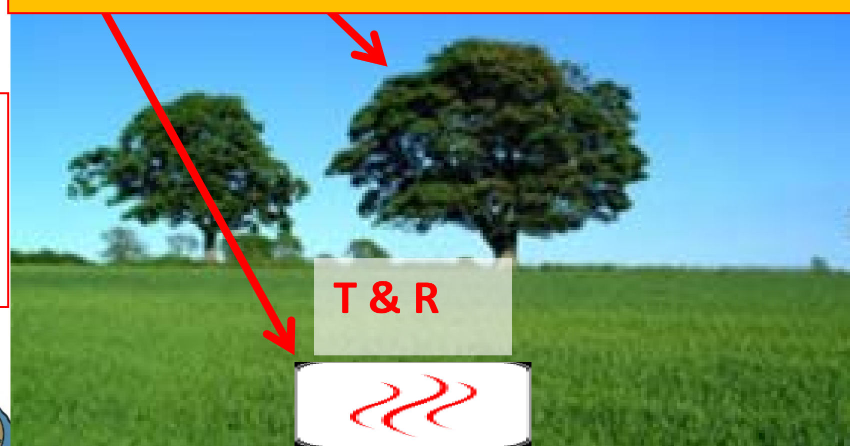

BVOC is a function of radiation and temperature

Satellite-Derived Insolation/PAR

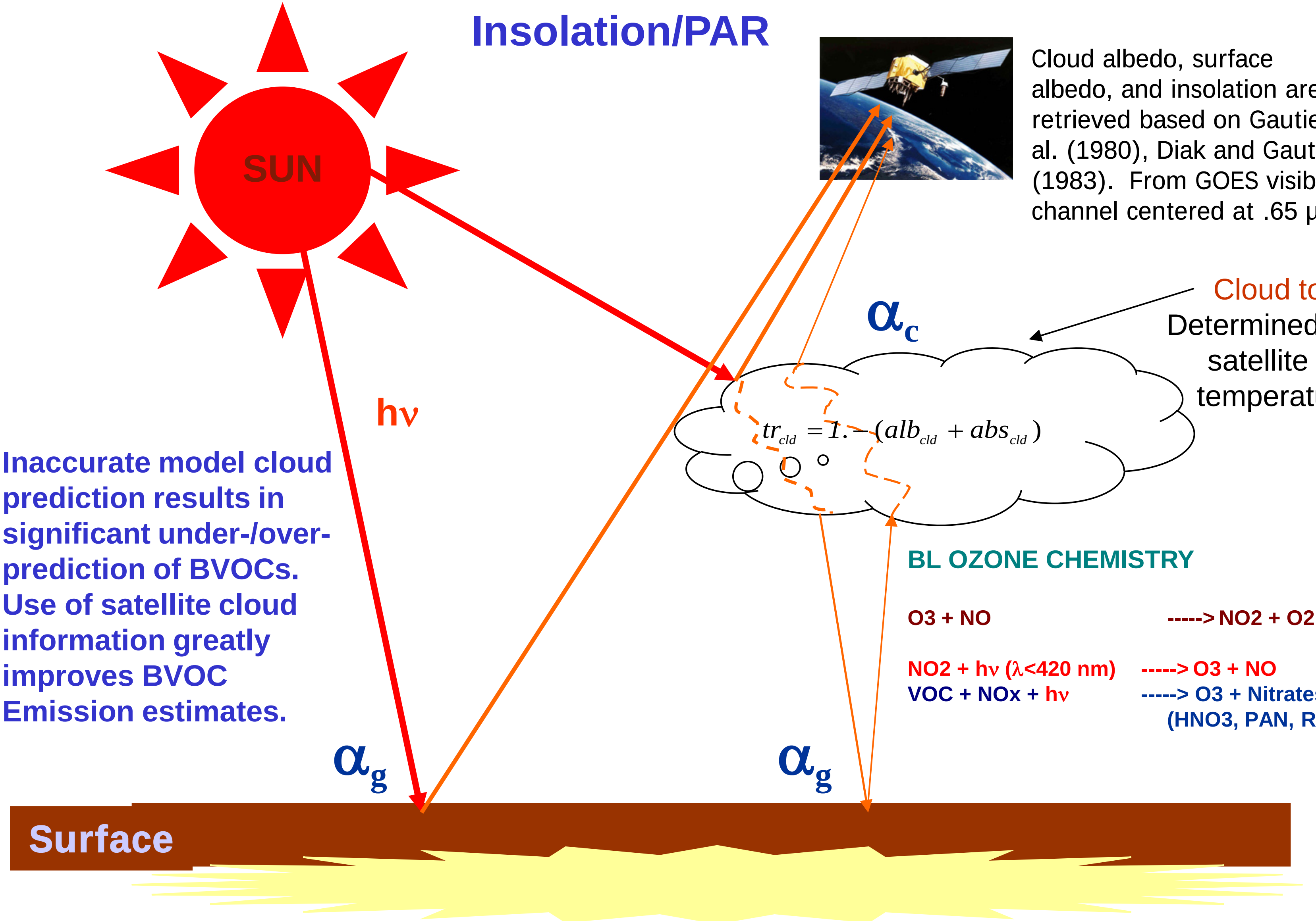

Cloud albedo, surface albedo, and insolation are retrieved based on Gautier et al. (1980), Diak and Gautier (1983). From GOES visible channel centered at .65 µm.

Cloud top
Determined from satellite IR temperature

Inaccurate model cloud prediction results in significant under-/over-prediction of BVOCs. Use of satellite cloud information greatly improves BVOC Emission estimates.

BL OZONE CHEMISTRY

O3 + NO -----> NO2 + O2

NO2 + hν (λ<420 nm) -----> O3 + NO
VOC + NOx + hν -----> O3 + Nitrates (HNO3, PAN, RONO2)

What is PAR?

$$PAR = \int_{.4}^{.7} I(\lambda)d\lambda \qquad (W\,m^{-2})$$

$$PAR = \frac{1}{hc}\int_{.4}^{.7} I(\lambda)d\lambda \qquad (quanta\,m^{-2}s^{-1})$$

- In most applications (e.g., agriculture related) a conversion factor CF is used:

$$CF = \frac{PAR}{Insolation}$$

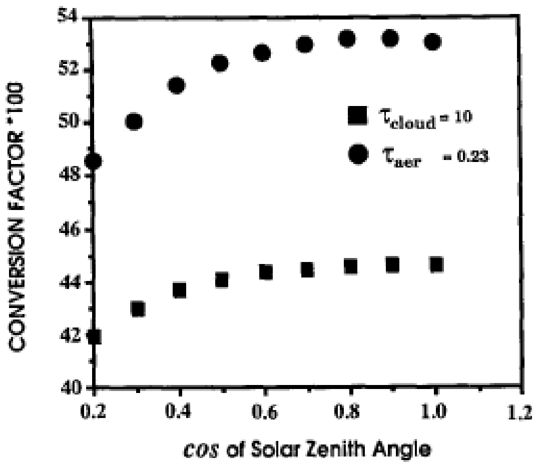

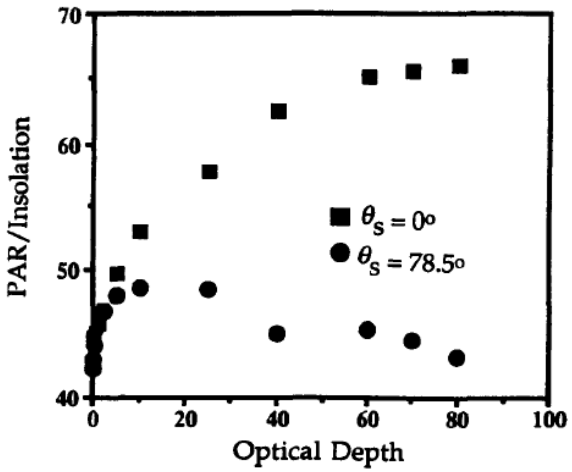

Direct and diffuse light differences: Highest sensitivity to clouds/aerosols and zenith angle, but not in the same direction. *(Adapted from: Frouin and Pinker, 1994; Pinker and Laszelo, 1991)*

Satellite-Derived Photosynthetically Active Radiation (PAR)

$$PAR = \int_{.4}^{.7} I(\lambda)d\lambda \quad (W\ m^{-2}) = \frac{1}{hc}\int_{.4}^{.7} I(\lambda)d\lambda \quad (quantam^{-2}s^{-1})$$
$$= Insolation \quad \times \quad CF$$

$$CF = \frac{PAR}{Insolation} = .42 + .28 * ODfactor * Zfactor$$

Based on Stephens (1978), Joseph (1976), Pinker and Laszlo (1992), Frouin and Pinker (1995)

$$\tau = \frac{8\alpha_c}{(1-\alpha_c)^2}, \quad where \qquad \alpha_c = cloud\ albedo$$

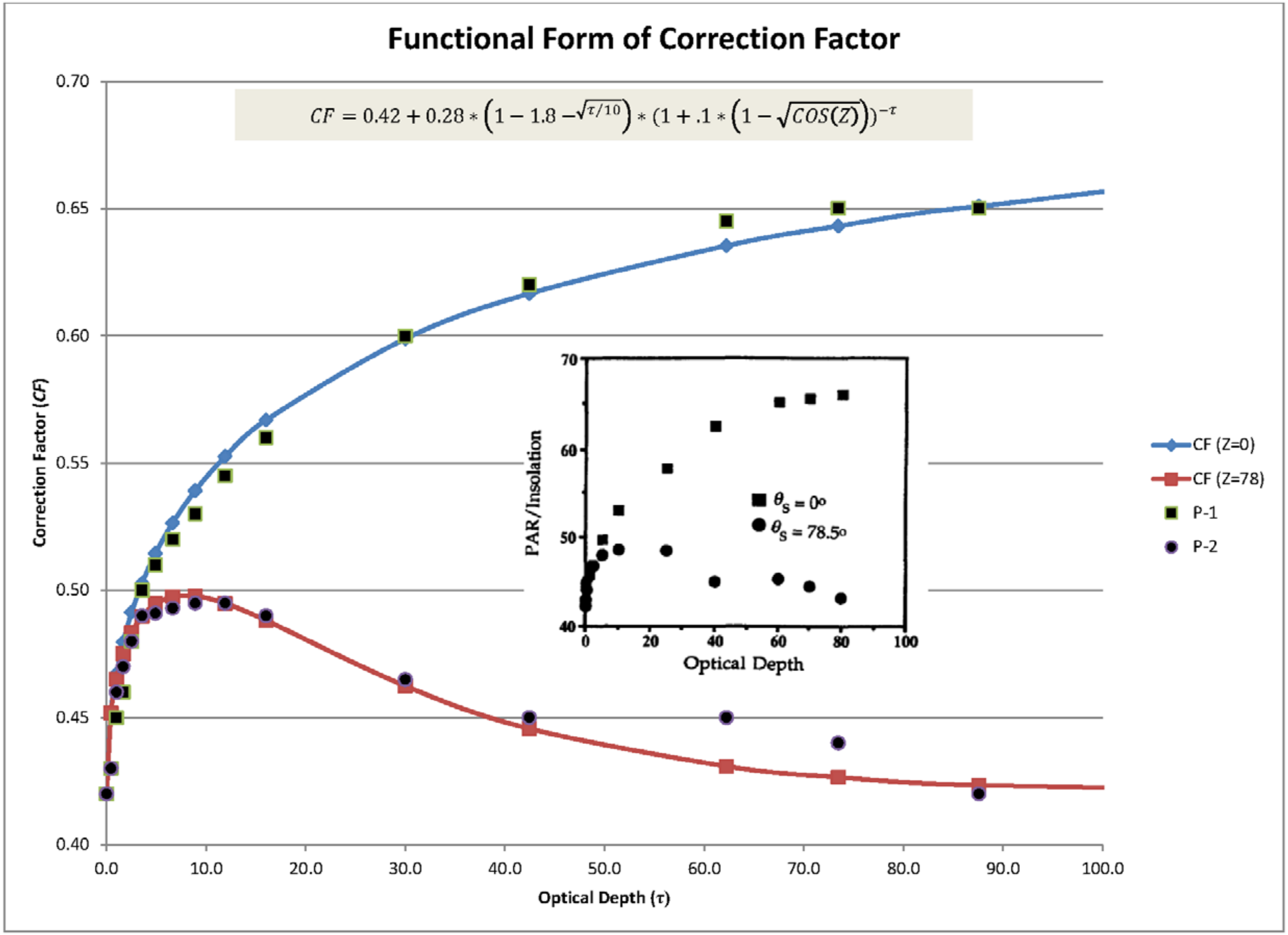

Functional Form of Correction Factor
$CF = 0.42 + 0.28 * \left(1 - 1.8^{-\sqrt{\tau/10}}\right) * \left(1 + .1 * \left(1 - \sqrt{COS(Z)}\right)\right)^{-\tau}$
Correction Factor (CF)
0.70
0.65
0.60
0.55
0.50
0.45
0.40
0.0
10.0
20.0
30.0
40.0
50.0
60.0
70.0
80.0
90.0
100.0
Optical Depth (τ)
CF (Z=0)
CF (Z=78)
P-1
P-2
PAR/Insolation
70
60
50
40
0
20
40
60
80
100
Optical Depth
$\theta_S = 0°$
$\theta_S = 78.5°$

Satellite-derived insolation and PAR for September 14, 2013, at 19:45 GMT.

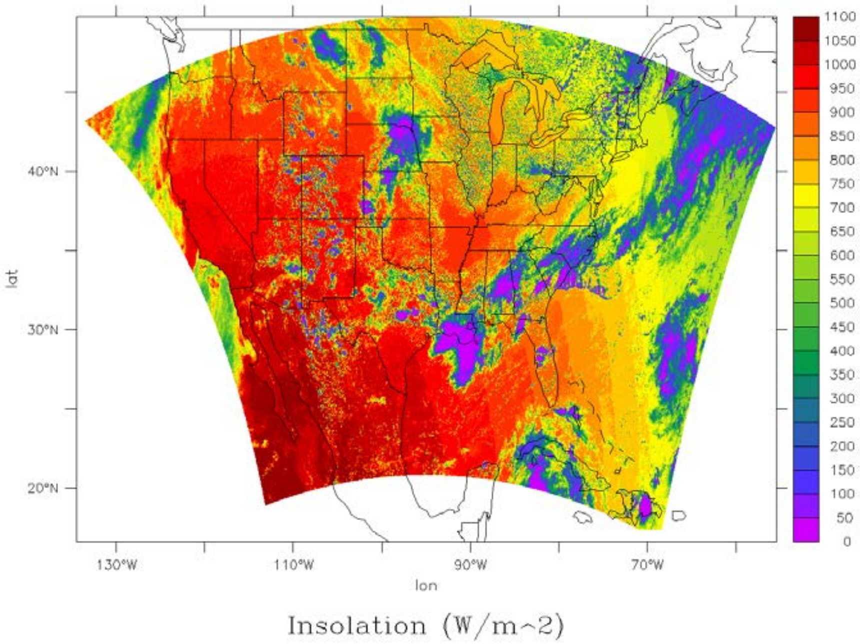

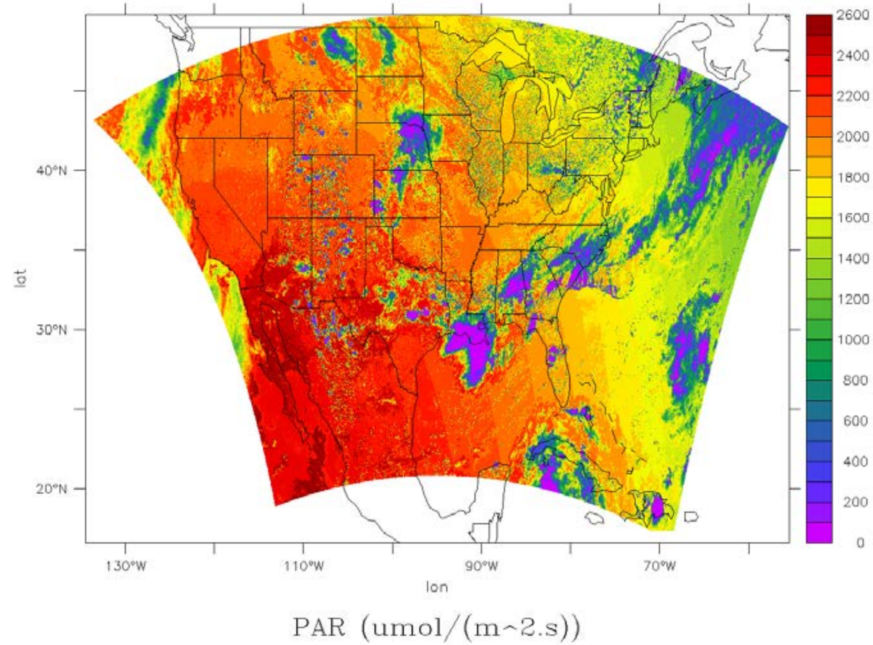

Insolation/PAR Evaluation

Spatial Distribution of NMB (normalized mean bias) Against Soil Climate Analysis Network (SCAN)

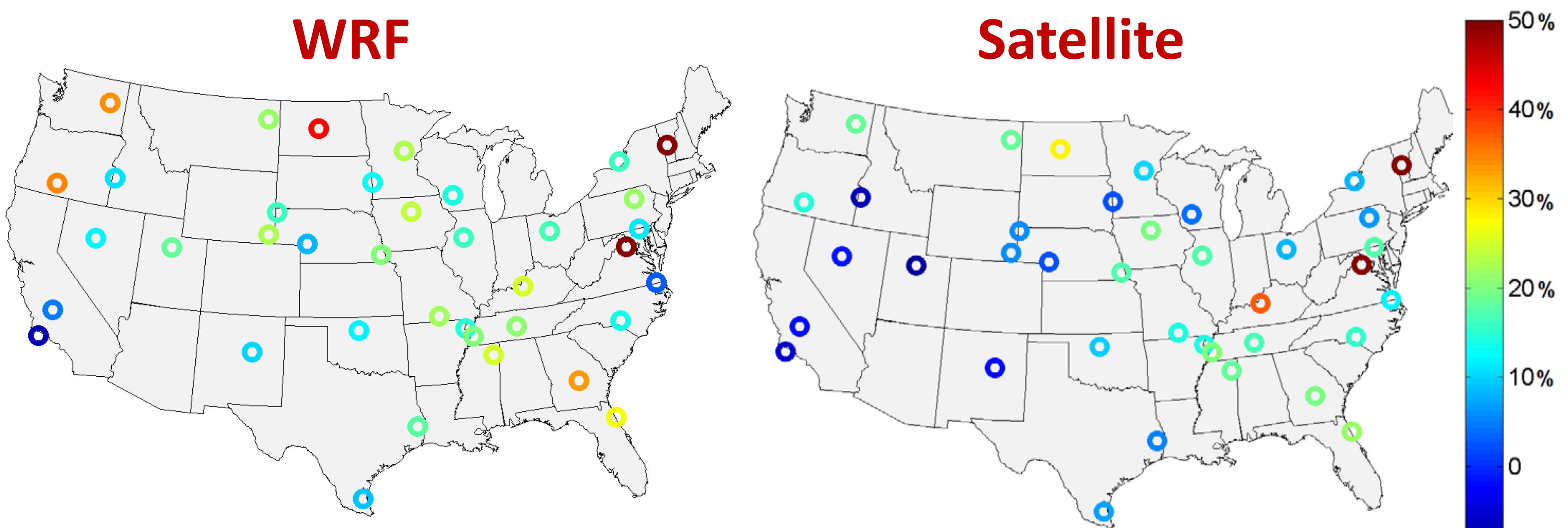

WRF
NMB = 22%
NME = 34%

Satellite
NMB = 14%
NME = 27%

GOES Insolation Bias Increases From West to East

- The clear sky bias is partly due to the lack of a dynamic precipitable water in retrieval algorithm.
- The retrievals will be re-processed to correct this issue.

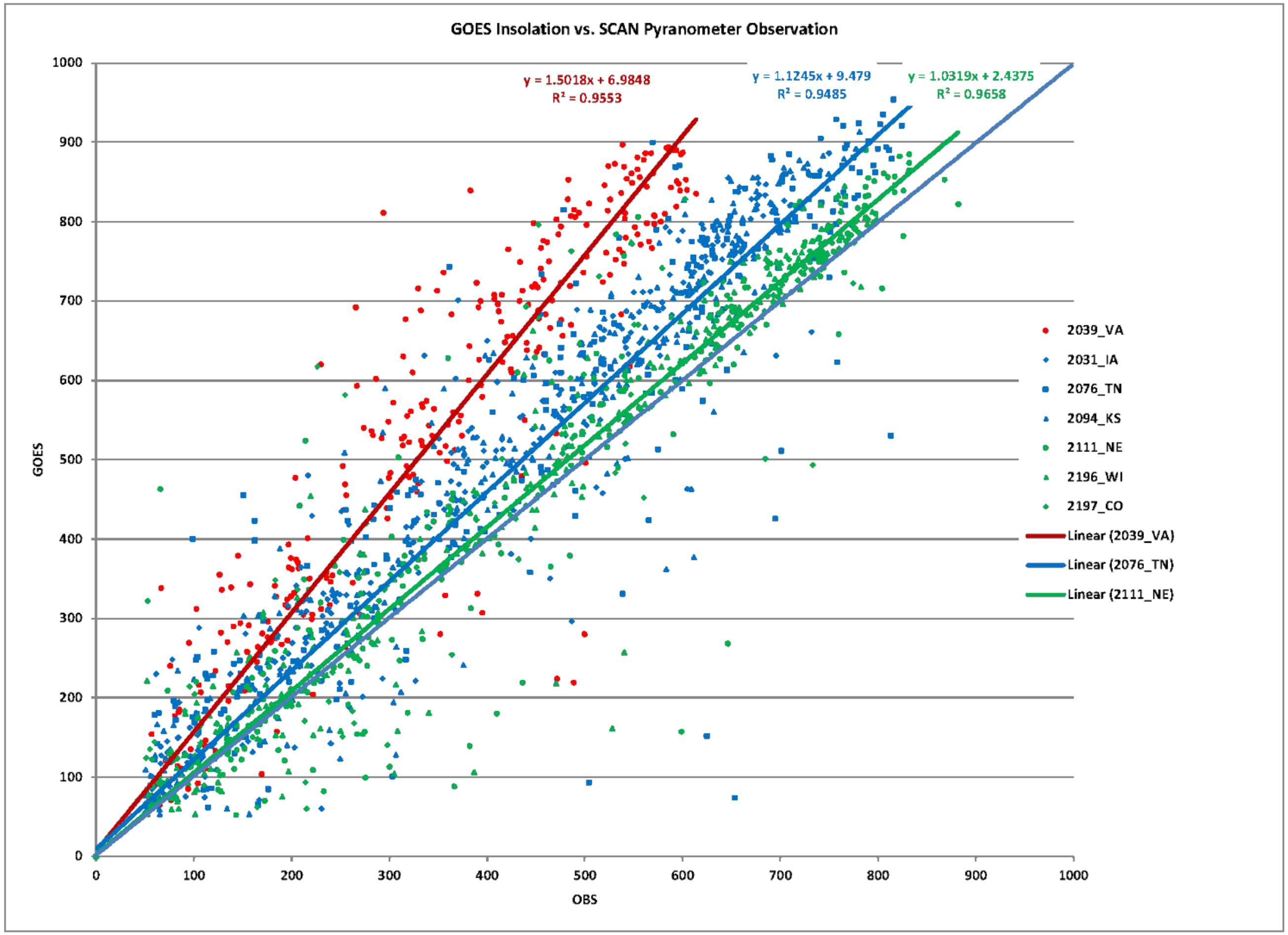

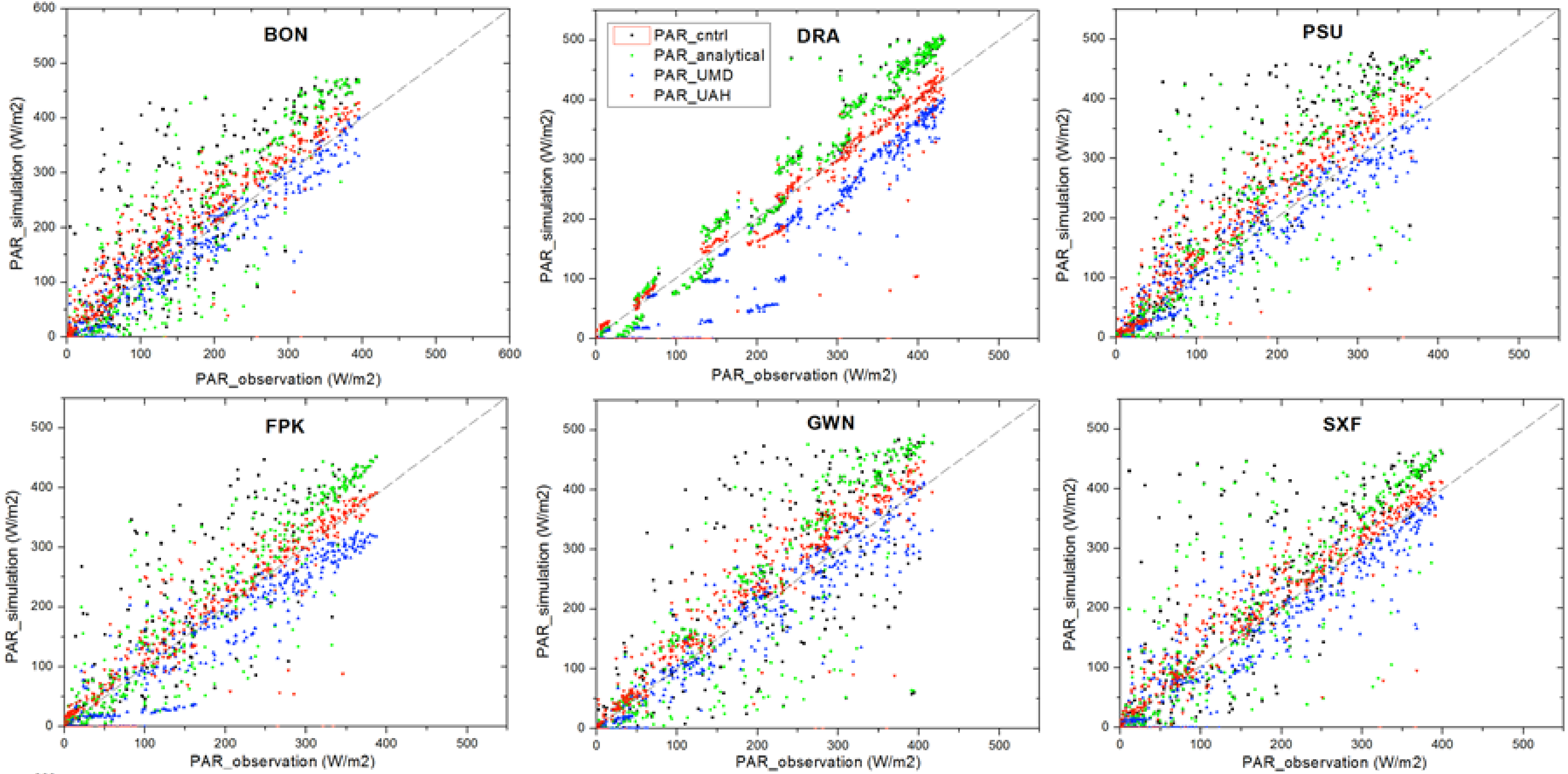

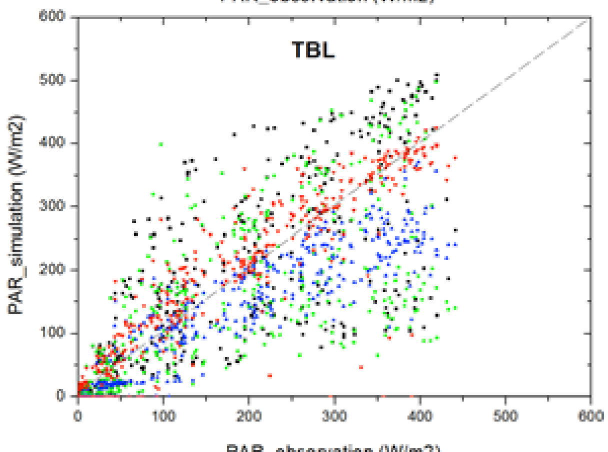

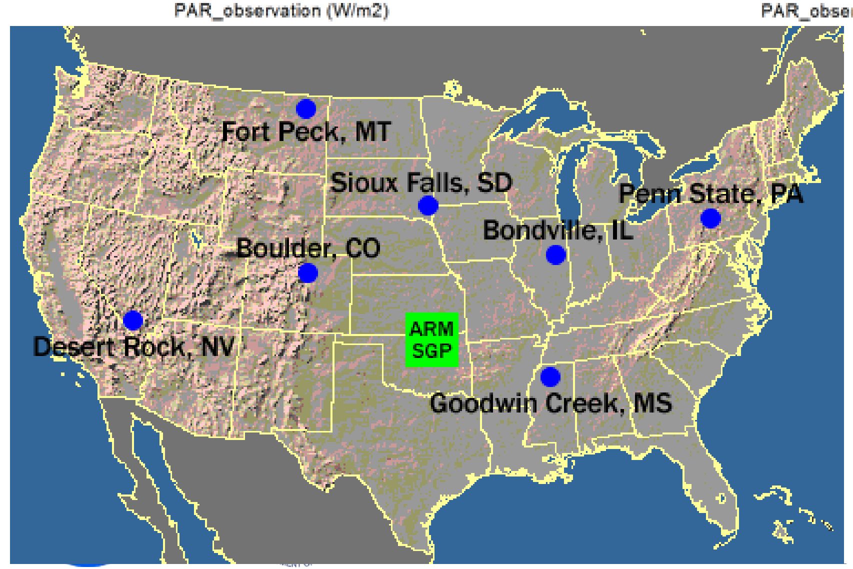

PAR evaluation against SURFRAD stations for August 2006. UAH product with bias correction shows the best agreement with surface obs.

Air Quality Management District

Resources Board

GEORGIA

TCEQ

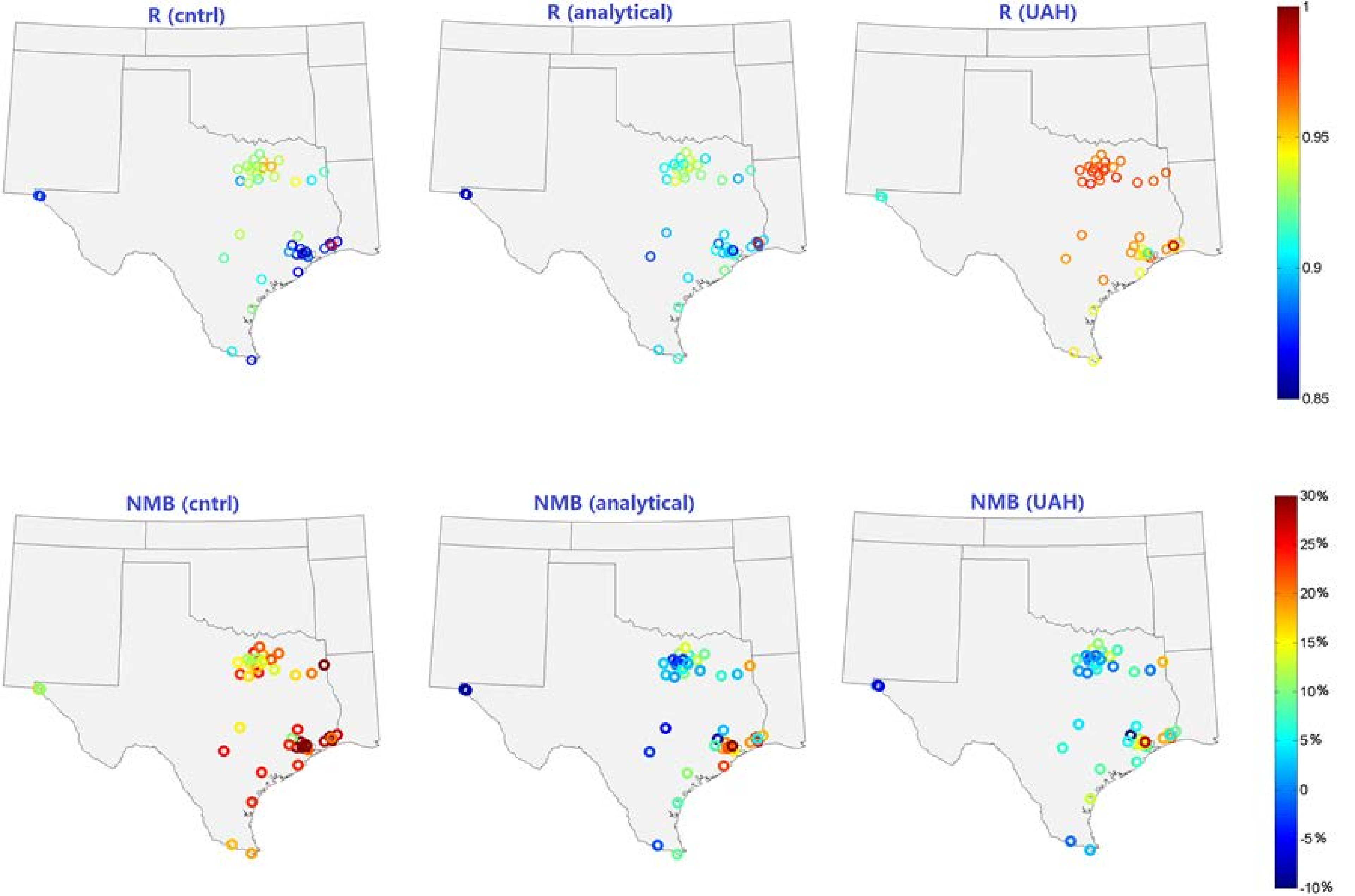

Comparing August, 2006, insolation from control WRF simulation (cntrl), UAH WRF simulation (analytical), and satellite-based (UAH) against 47 radiation monitoring stations in Texas.

Satellite-derived PAR substantially reduced isoprene emission estimates over Texas (DISCOVER-AQ period)

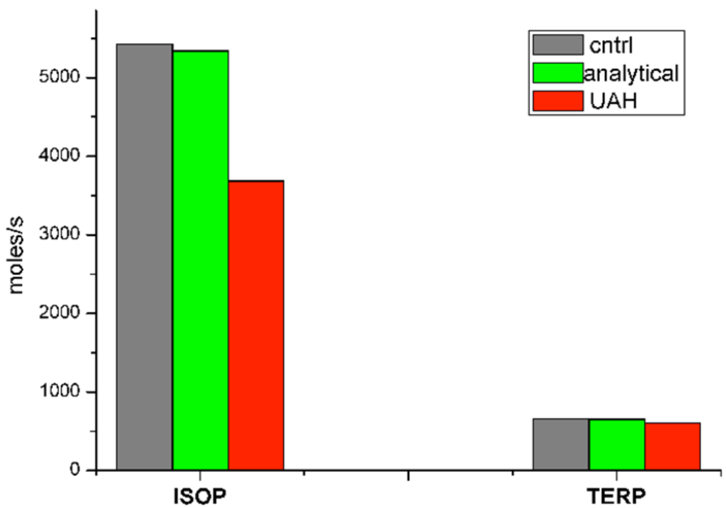

Domain-wide sum of estimated isoprene (ISOP) and monoterpene (TERP) emission strength over Texas area using different PAR inputs in MEGAN during September 2013.

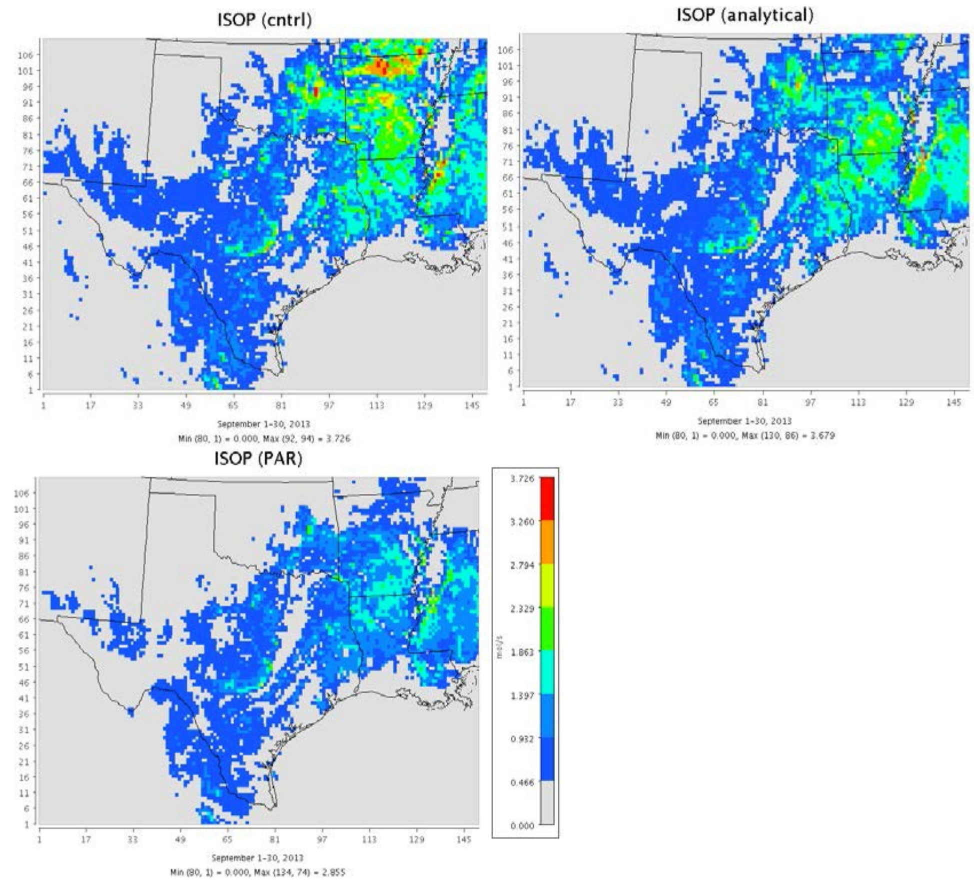

Comparison of the spatial pattern of estimated average isoprene emission rate in MEGAN using different PAR inputs over Texas domain during September 2013.

Estimated Emission Difference and Impact on O3 for September 2013 (Satellite - WRF)

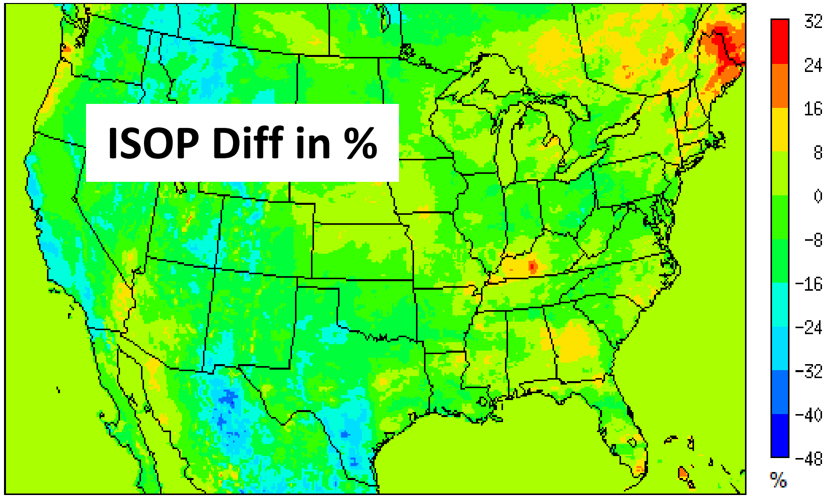

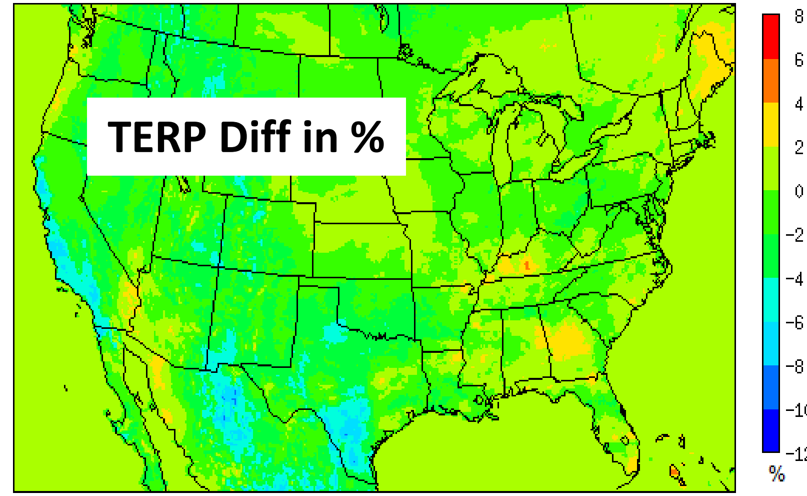

Isoprene emission is more sensitive to PAR inputs with the highest increase region at Northeast (>30%) and decrease at the Southwest (> 20%). The relative change for monoterpene emission is modest (-10% to 5%).

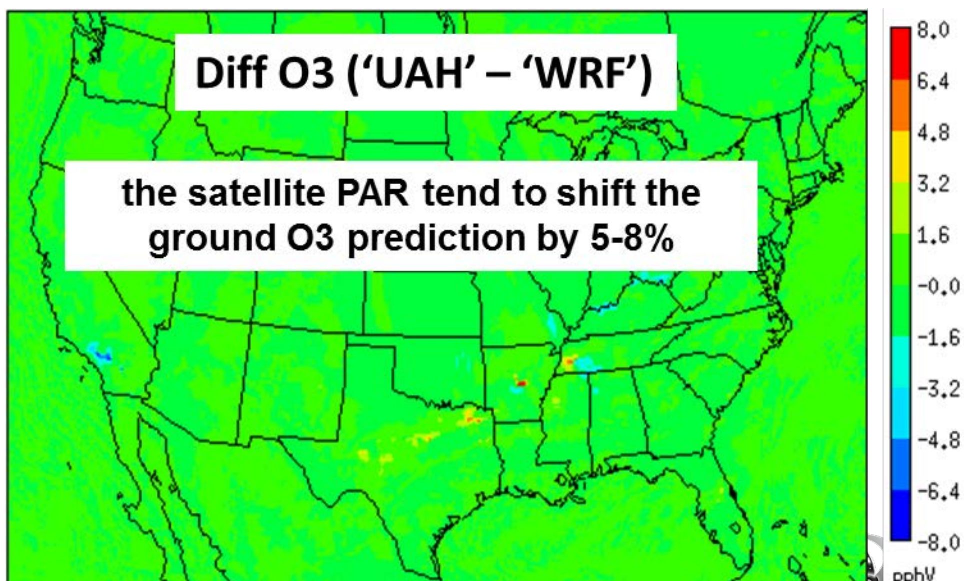

Bay Area Air Quality Management District
California Air Resources Board
Georgia
TCEQ
RICE
The University of Alabama in Huntsville

Mixing Heights – Underestimating mixing heights can cause overestimation of the sensitivity of controls. Emission reductions confined to a smaller volume cause a larger reduction in pollutants. A 30% error in mixing heights can produce 30% error in emission change impacts

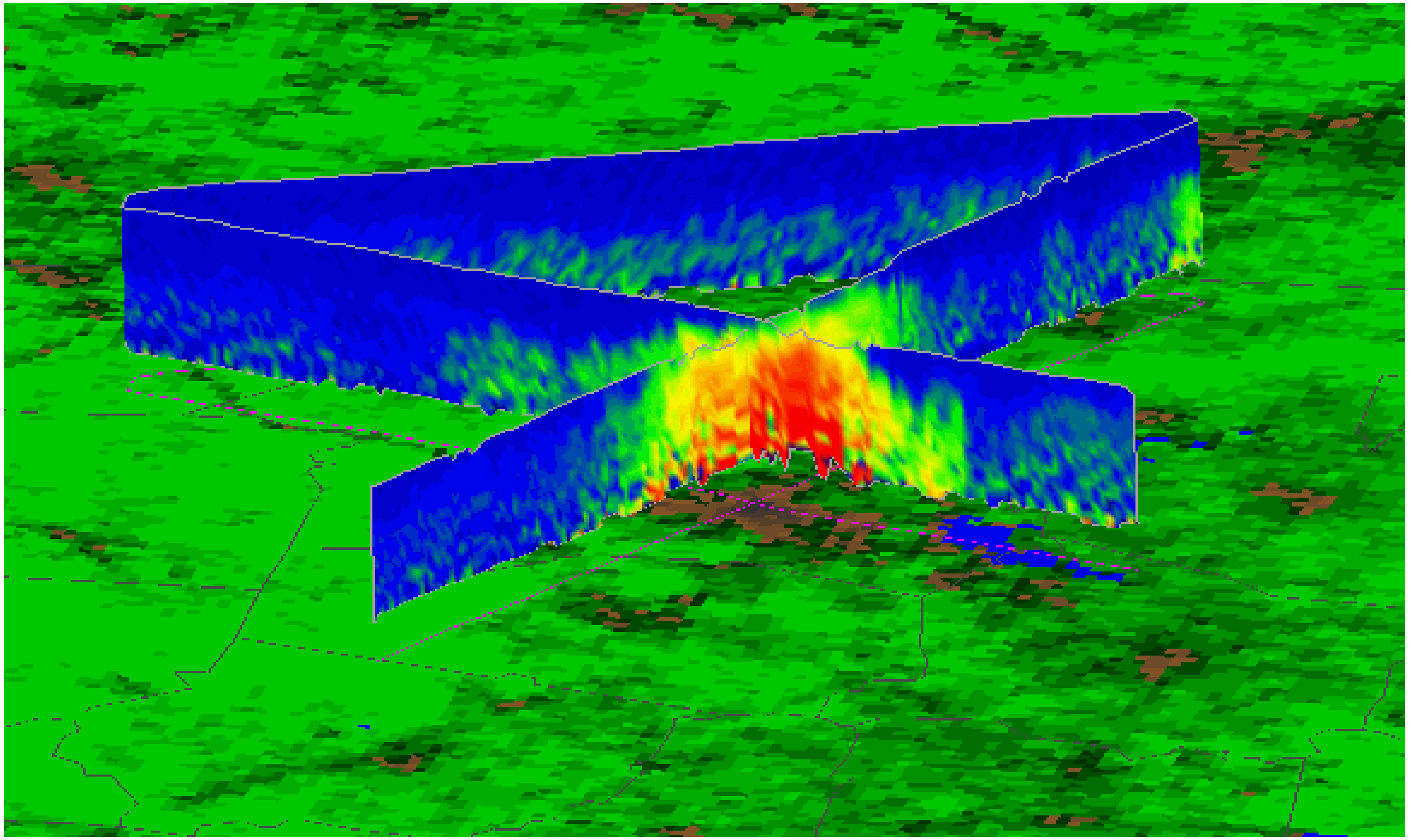

Can we perhaps use satellite observed skin temperatures to specify parameters in land use classes so that the model in turn reproduces the observed skin temperatures

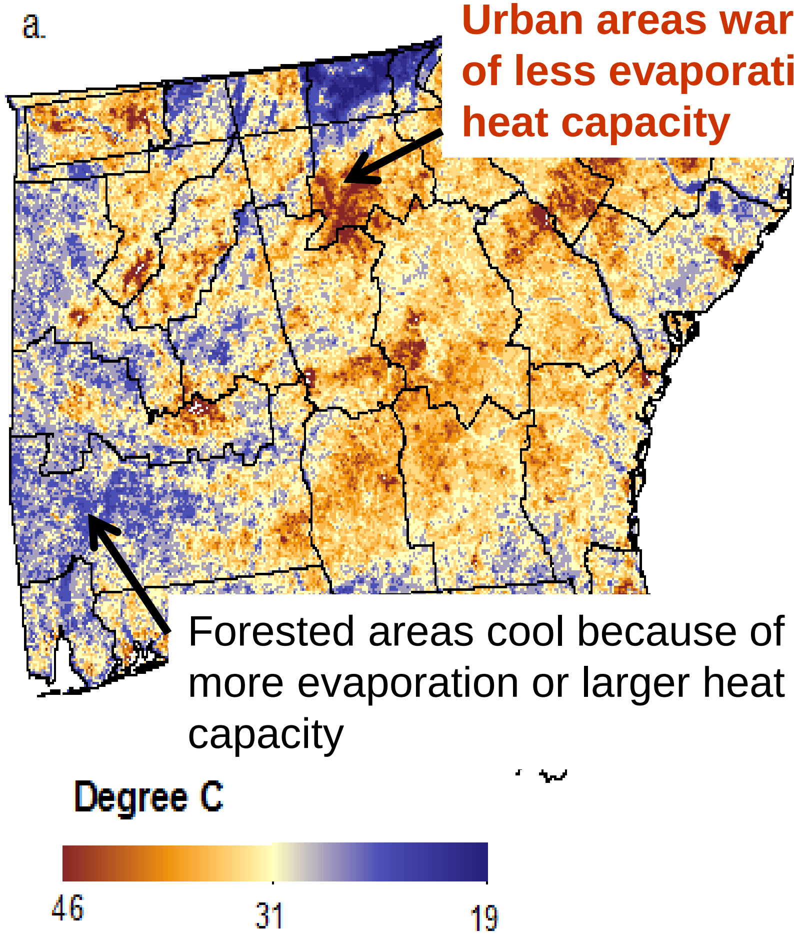

Urban areas warmer because of less evaporation or smaller heat capacity

Forested areas cool because of more evaporation or larger heat capacity

MODIS Skin Temperatures

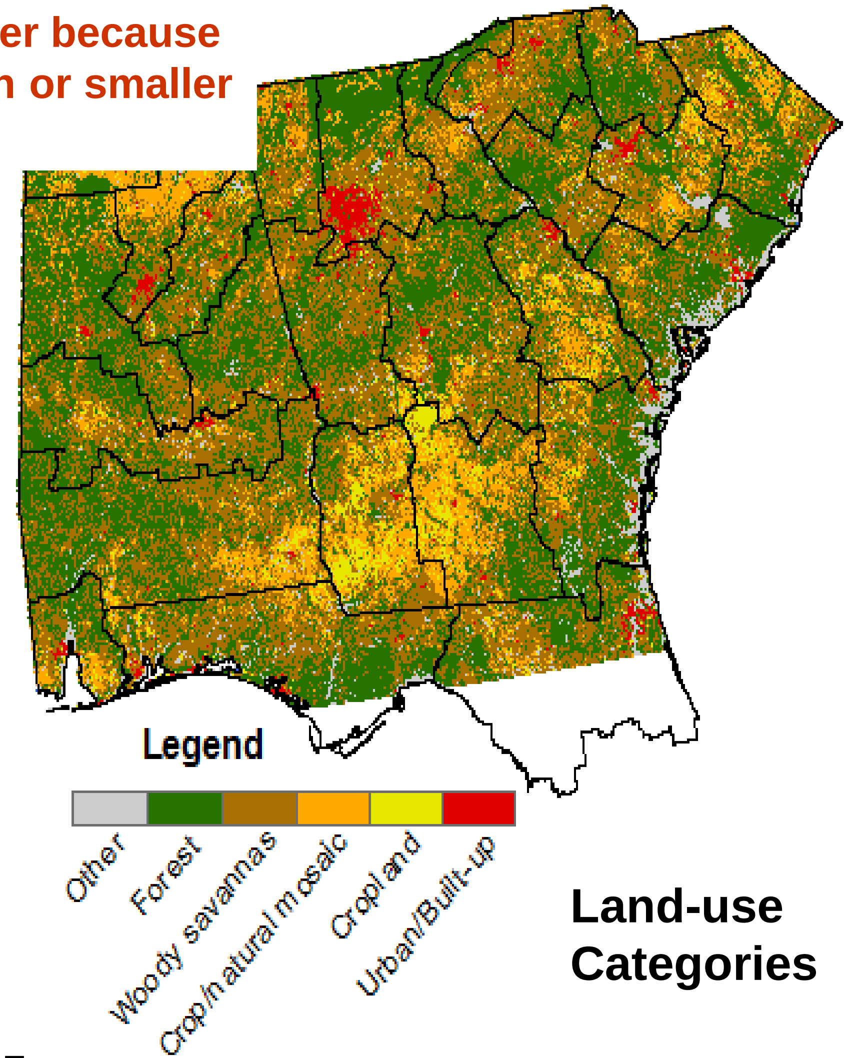

Land-use Categories

From Ellenburg 2015

Here we will constrain the Pleim-Xiu scheme with satellite data

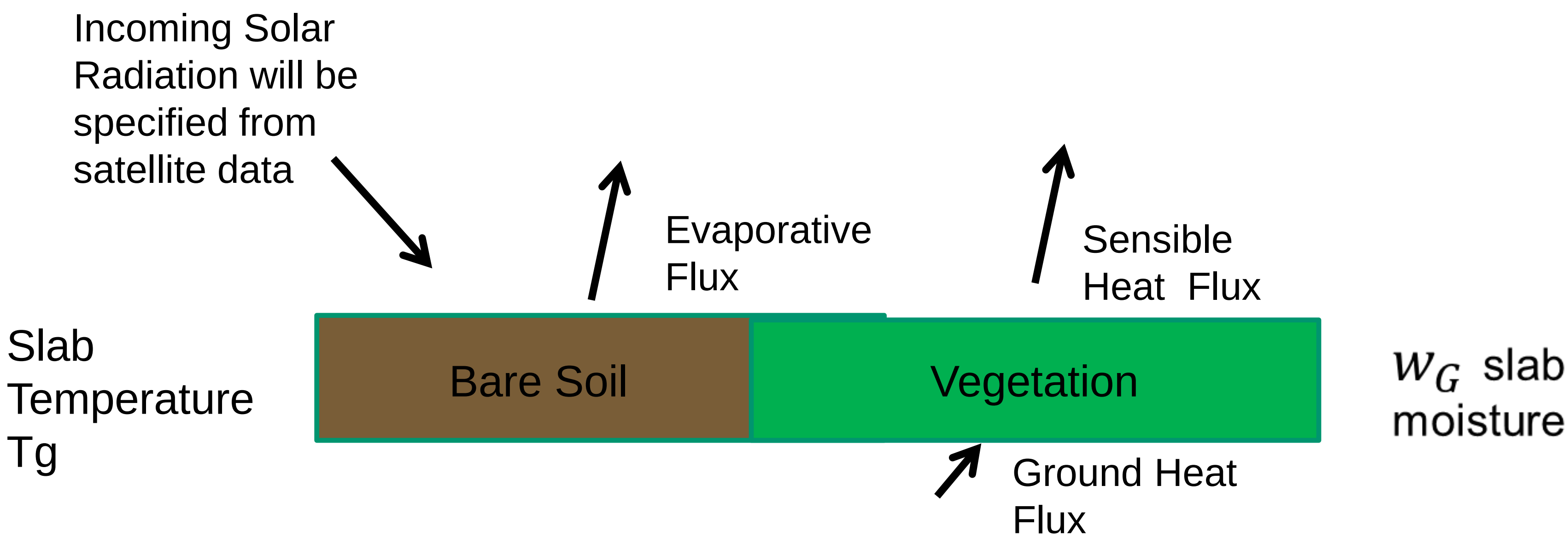

We will use differences between satellite skin temperature observations and model skin temperatures to nudge moisture in the proper direction.

$$\Delta w_G = \beta_1 (T_S^{Mod} - T_S^{Sat})_{Morning}$$

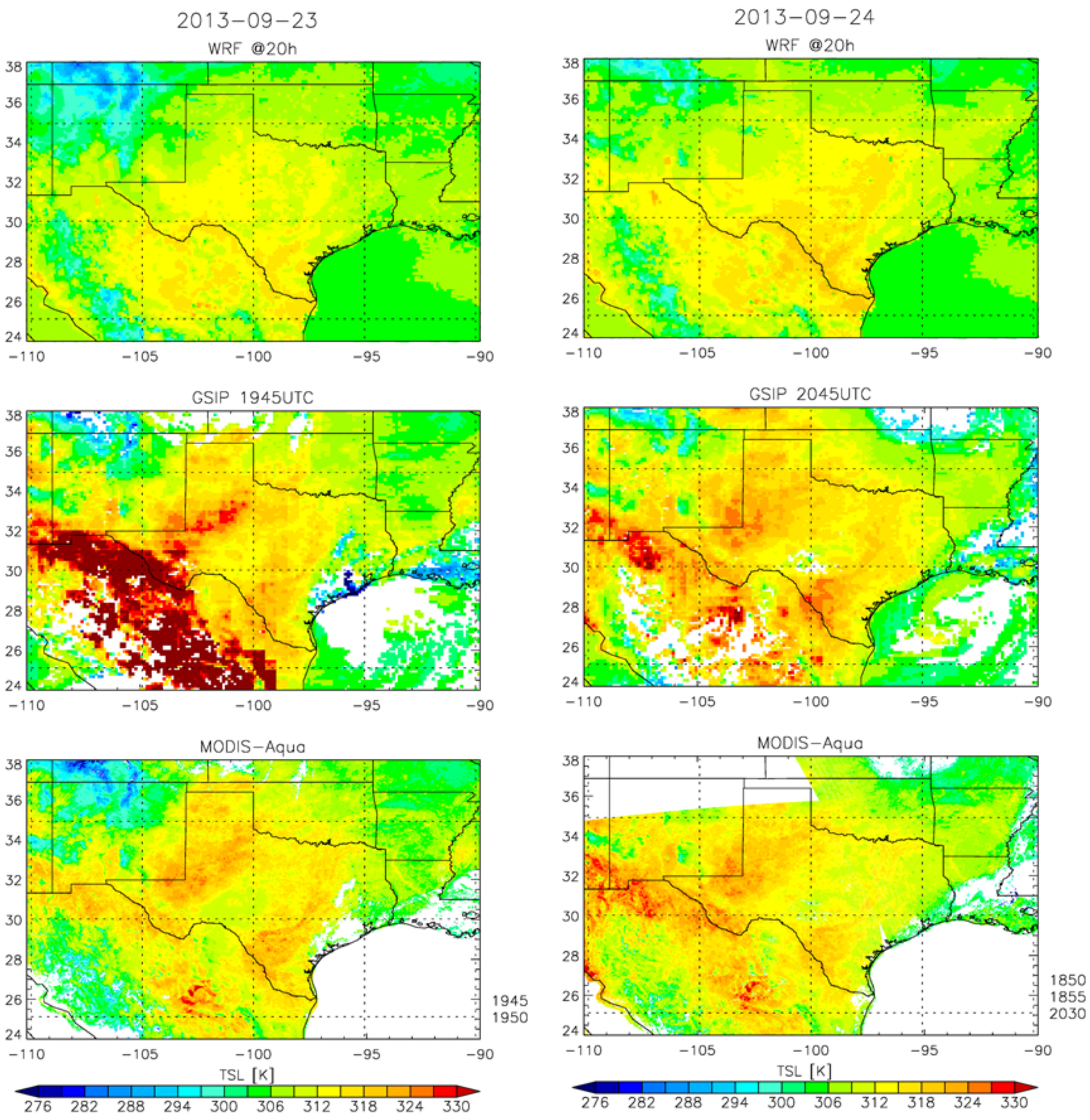

NOAA GSIP skin temperature product is too high in the West.

Skin Temperature, from top to bottom—WRF, GSIP, and MODIS(Aqua). Left panels are for Sep 23, 2013 (Aqua overpass time was 19:45&19:50 GMT), right panels for Sep 24, 2013 (main Aqua overpass time was 20:30 GMT).

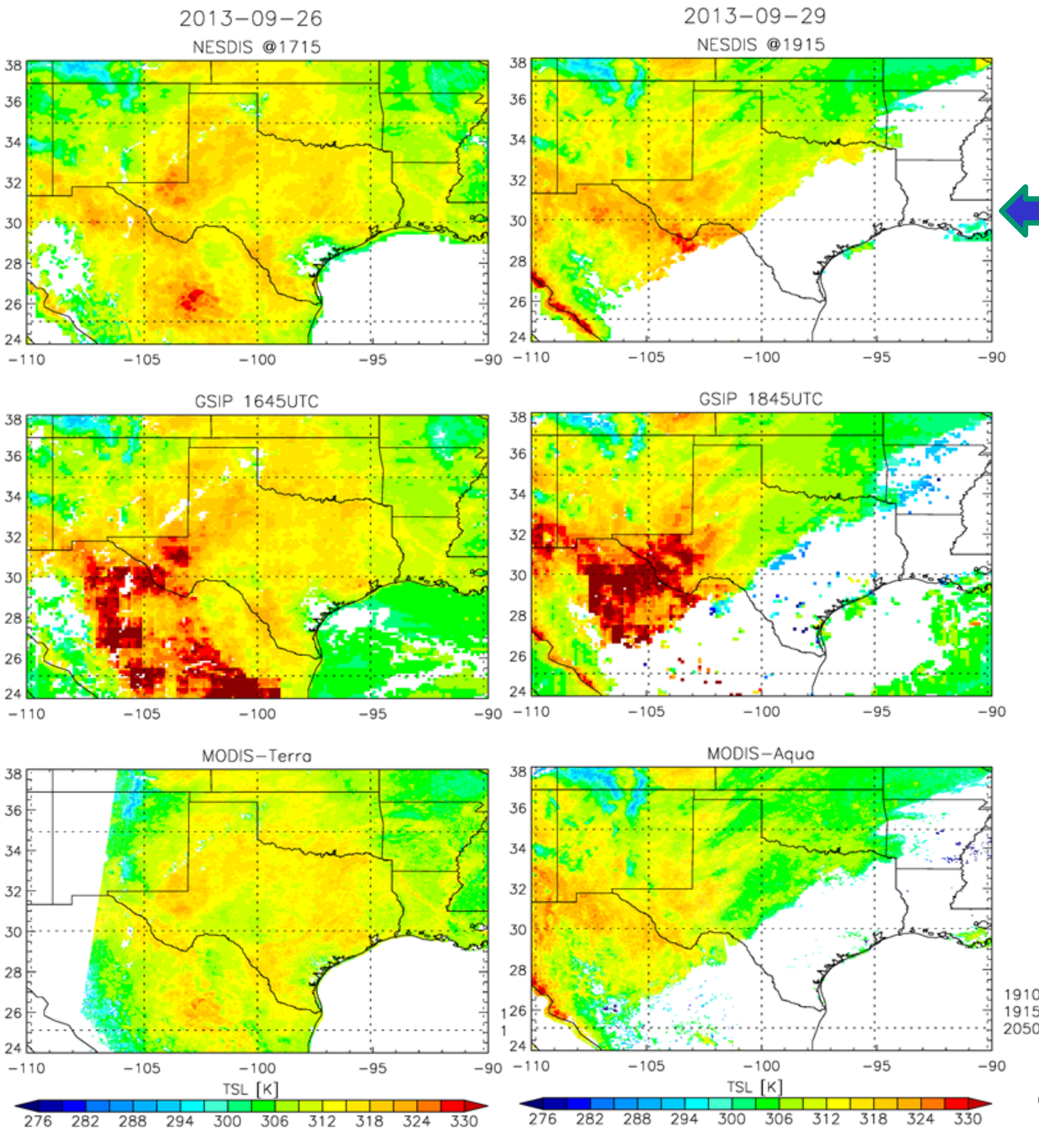

Comparison of NOAA ALEXI skin temperature product with GSIP and MODIS for September 26 and September 29. Top panel is the NOAA/ALEXI product. Middle panel is the GSIP product and bottom is the MODIS

NOAA/USDA ALEXI group (Anderson et al. 2007a and Anderson et al. 2007b).

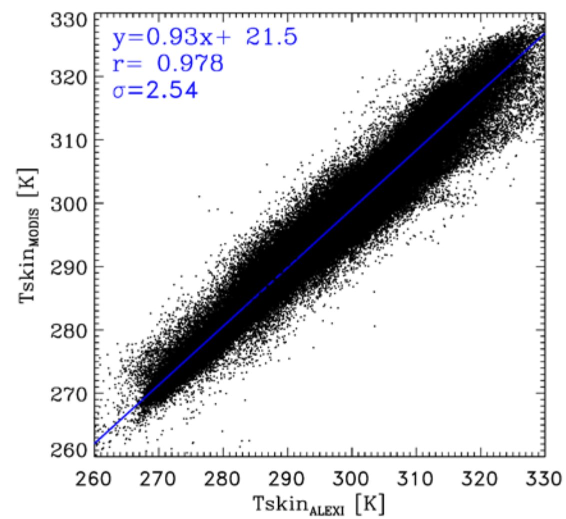

Comparison of Tskin from MODIS versus Tskin from the ALEXI product for all hours when data was available for the month of September 2013. This illustrates what may be the irreducible uncertainty in using skin temperatures as a model evaluation metric.

Bay Area Air Quality Management District
California Air Resources Board
Georgia
TCEQ
NASA
NOAA
NSSTC
RICE
The University of Alabama in Huntsville

CONCLUDING REMARKS

- Use of Satellite-based PAR in MEGAN model improved BVOC emission estimates and thus CMAQ performance during the DISCOVER-AQ Houston Campaign period in September 2013.
- The impact of PAR inputs on ozone prediction depends on the local NOx/VOC ratio. Over the VOC limited region, the satellite PAR tend to shift the ground O3 prediction by 5-8%.
- Currently we are in the process of producing and archiving PAR for 2006-present with the new (updated) retrieval code. The new retrieval system uses a dynamic moisture field, thus, partly correcting PAR over-estimation in the eastern United States.
- We are still evaluating skin temperature assimilation technique over Texas.
- The work presented here will be expanded and tested over California involving our California partners.

Acknowledgment

The findings presented here were accomplished under partial support from NASA Science Mission Directorate Applied Sciences Program and the Texas Air Quality Research Program (T-AQRP).

Note the results in this study do not necessarily reflect policy or science positions by the funding agencies.

Thank You

Future Tasks

- Resolve the issues with CMAS and hold a workshop.
- Complete transitioning to CMAS and TCEQ.
  - Complete documentation.
  - Work with TCEQ for independent evaluation of tools and techniques.
- Upgrade the current web based data delivery system for the new data format.
- Respond to user community's request for Photosynthetically Active Radiation (PAR).
  - We had requests from Dave Allen's group at University of Texas-Austin, Russ Dickerson at University of Maryland and Rice University.

ADDITIONAL SLIDES

ACRONYMS

CMAQ	EPA's Community Multiscale Air Quality (CMAQ) Model
CMAS	Community Modeling and Analysis System
EPA	Environmental Protection Agency
LNOx	Lightning Generated Nitrogen Oxides
LNOM	Lightning Nitrogen Oxides Model
NASA	National Aeronautics and Space Administration
SIP	State Implementation Plan
TCEQ	Texas Commission on Environmental Quality

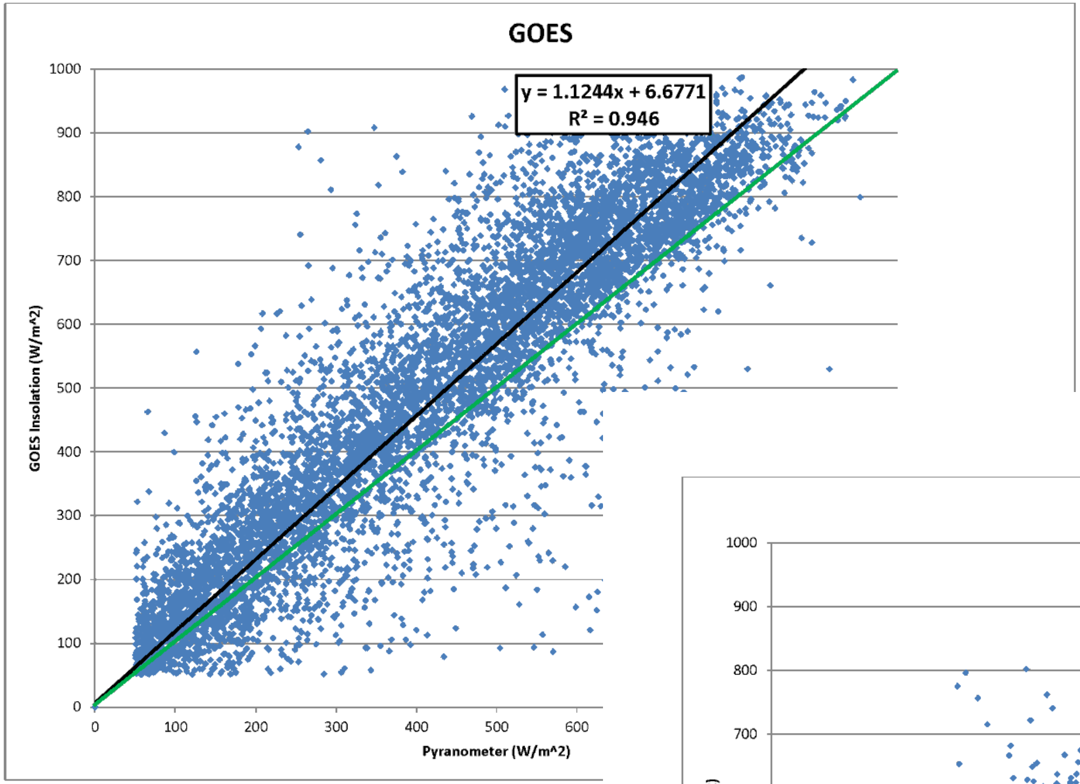

Performing bias correction before converting to PAR

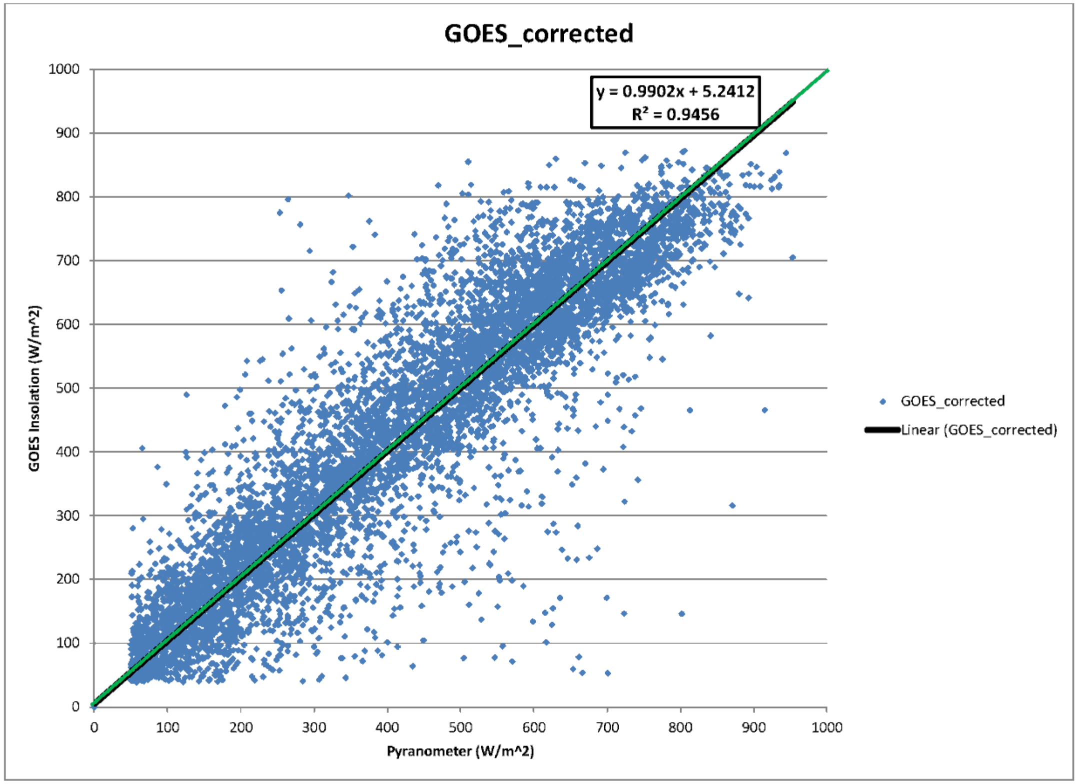

Response for Daily Max 8-hr Average O3 concentrations (September 2013)

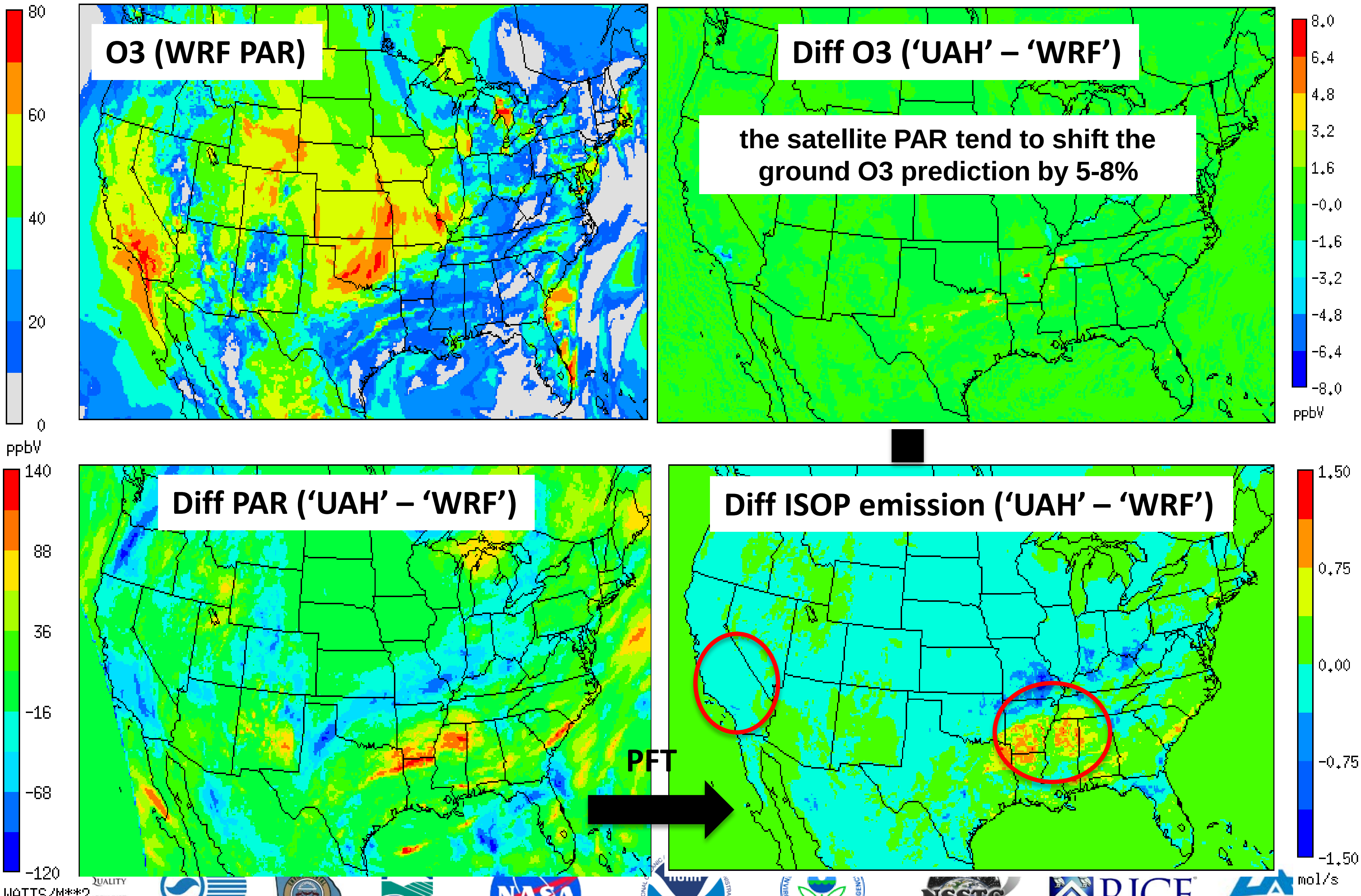

Temperature and Moisture Modeling

Factors controlling surface temperatures and moisture are complex and many models have created complex land surface models that in the end require many ill defined parameters.

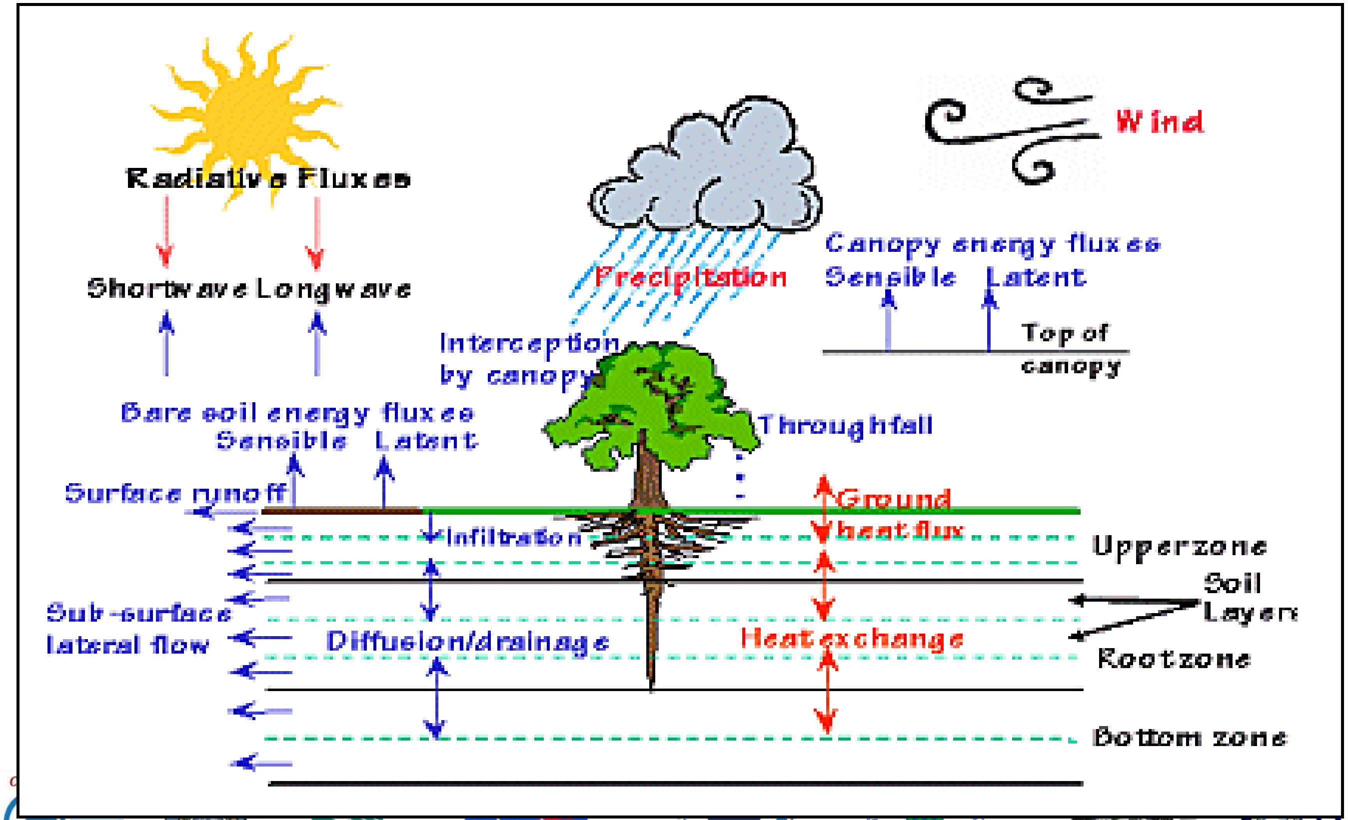

Models have attempted to improve performance by developing improved land use classes (LUC) using in situ and satellite data

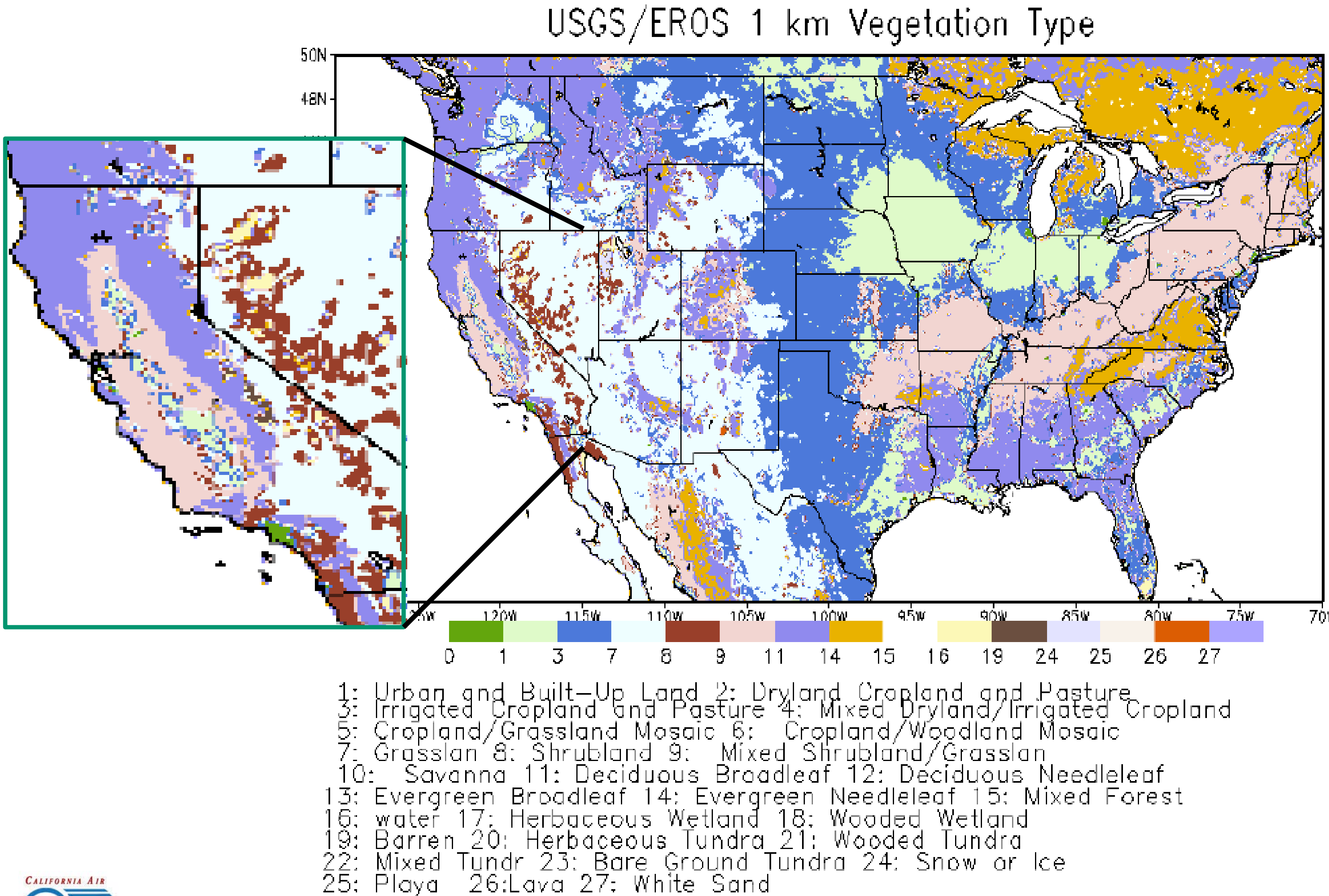

Bay Area Air Quality Management District

California Air Resources Board

GEORGIA

TCEQ

THE UNIVERSITY OF ALABAMA IN HUNTSVILLE

Unfortunately models don't use land surface classes directly. Physical parameters such as heat capacity, canopy resistance, surface moisture have to be defined for the Land Use Class

Vegetation Parameters

Albedo - SFC albedo (in percentage)	RGL - Parameter used in radiation stress function
Z0 – Roughness Length (m)	HS - Parameter used in vapor pressure deficit
SHDFAC - Green vegetation fraction	SNUP - Threshold depth for 100% snow cover
NROOT - Number of root layers	LAI - Leaf area index (dimensionless)
RS - stomatal resistance (s m-1)	MAXALB - Upper bound on max albedo snow

Category	Class	Albedo	Z0	SHDFAC	NROOT	RS	RGL	HS	SNUP	LAI	MAXALB
Urban and Built-Up Land	1	0.15	1.00	0.10	1	200.	999.	999.0	0.04	4	40
Dryland Cropland and Pasture	2	0.19	0.07	0.80	3	40.	100.	36.25	0.04	4	64
Irrigated Cropland and Pasture	3	0.15	0.07	0.80	3	40.	100.	36.25	0.04	4	64
Mixed Dryland/Irrigated Cropland and Pasture	4	0.17	0.07	0.80	3	40.	100.	36.25	0.04	4	64
Cropland/Grassland Mosaic	5	0.19	0.07	0.80	3	40.	100.	36.25	0.04	4	64
Cropland/Woodland Mosaic	6	0.19	0.15	0.80	3	70.	65.	44.14	0.04	4	60
Grassland	7	0.19	0.08	0.80	3	40.	100.	36.35	0.04	4	64
Shrubland	8	0.25	0.03	0.70	3	300.	100.	42.00	0.03	4	69
Mixed Shrubland/Grassland	9	0.23	0.05	0.70	3	170.	100.	39.18	0.035	4	67
Savanna	10	0.20	0.86	0.50	3	70.	65.	54.53	0.04	4	45
Deciduous Broadleaf Forest	11	0.12	0.80	0.80	4	100.	30.	54.53	0.08	4	58
Deciduous Needleleaf Forest	12	0.11	0.85	0.70	4	150.	30.	47.35	0.08	4	54
Evergreen Broadleaf Forest	13	0.11	2.65	0.95	4	150.	30.	41.69	0.08	4	32
Evergreen Needleleaf Forest	14	0.10	1.09	0.70	4	125.	30.	47.35	0.08	4	52
Mixed Forest	15	0.12	0.80	0.80	4	125.	30.	51.93	0.08	4	53
Water Bodies	16	0.19	0.001	0.00	0	100.	30.	51.75	0.01	4	70
Herbaceous Wetland	17	0.12	0.04	0.60	2	40.	100	60.00	0.01	4	35
Wooded Wetland	18	0.12	0.05	0.60	2	100.	30.	51.93	0.02	4	30
Barren and Sparsely Vegetated	19	0.12	0.01	0.01	1	999.	999.	999.0	0.02	4	69
Herbaceous Tundra	20	0.16	0.04	0.60	3	150.	100.	42.00	0.025	4	58
Wooded Tundra	21	0.16	0.06	0.60	3	150.	100.	42.00	0.025	4	55
Mixed Tundra	22	0.16	0.05	0.60	3	150.	100.	42.00	0.025	4	55
Bare Ground Tundra	23	0.17	0.03	0.30	2	200.	100.	42.00	0.02	4	65
Snow or Ice	24	0.70	0.001	0.00	1	999.	999.	999.0	0.02	4	75

Climate models must use complex models for energy and water balance models to run unattended for years.

In weather forecasting and air pollution applications the better approach may be to use simple models highly constrained by observations.

This may be especially true for retrospective studies such as SIP periods.

Examples

McNider et al 1994 MWR Moisture adjustment using satellite time tendency data

Anderson et al 1997(ALEXI) JAM moisture adjustment using satellite data

Pleim and Xiu 2003 JAM Moisture adjustment using surface obs

McNider et al 2005 JCAM Heat capacity/thermal inertia adjustment.

The satellite observes a skin or radiating temperature while the original Pleim-Xiu scheme only provided a slab temperature associated with a finite heat capacity - c_g

$$c_g \frac{\partial T_G}{\partial t} = R_L + (1 - \alpha_s) R_s - \varepsilon \sigma T_S^4 - H - E - G$$

Following Makaro 2011 we take the limit of c_g approaching 0 to obtain a infinitely thin surface.

$$R_L + (1 - \alpha_s) R_s - \varepsilon \sigma T_S^4 - H - E - S = 0$$

We use root finding techniques to recover a true skin temperature, T_s .

We have taken a different approach and have embraced simple models but highly constrained by observations. Simple model is based on the Pleim-Xiu scheme in WRF.

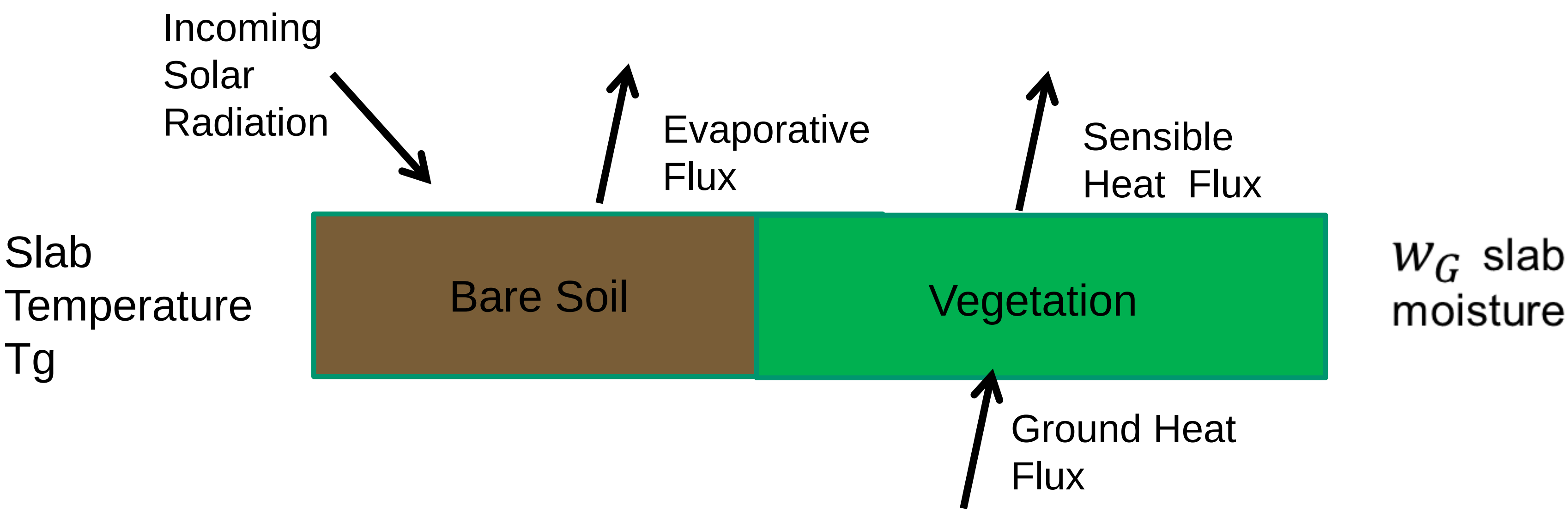

Original Pleim-Xiu used differences between National Weather Service observations and model temperatures to nudge moisture in the proper direction.

$$\Delta w_G = \alpha_1 (T_S^F - T_S^A) + \alpha_2 (RH^F - RH^A)\ _{Daytime}$$

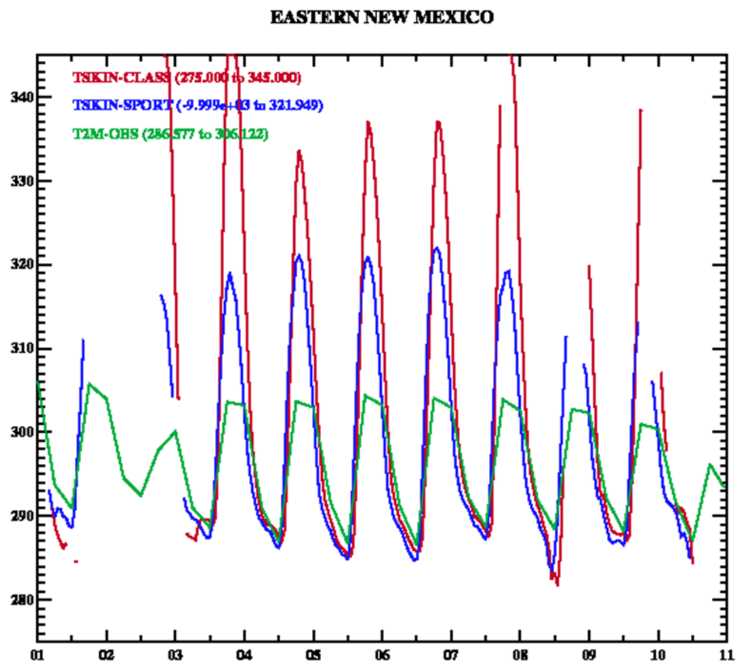

Time series for the first part of September 2013 showing GSIP skin temperatures, SPoRT skin temperatures and 2m observed temperature.

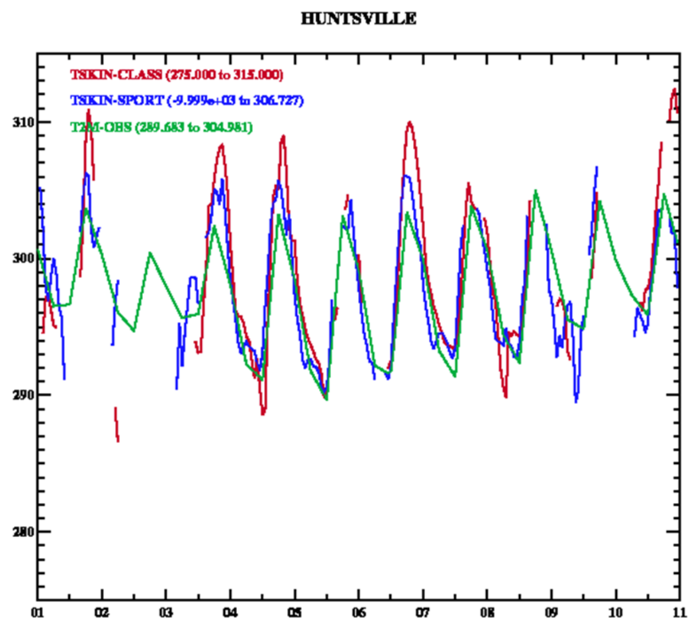

Time series for the first part of September 2013 showing GSIP skin temperatures, SPoRT skin temperatures and 2m observed temperature.

BAY AREA AIR QUALITY MANAGEMENT DISTRICT · CALIFORNIA AIR RESOURCES BOARD · GEORGIA · TCEQ · NASA · NOAA · UNITED STATES ENVIRONMENTAL PROTECTION AGENCY · NSSTC · RICE · THE UNIVERSITY OF ALABAMA IN HUNTSVILLE

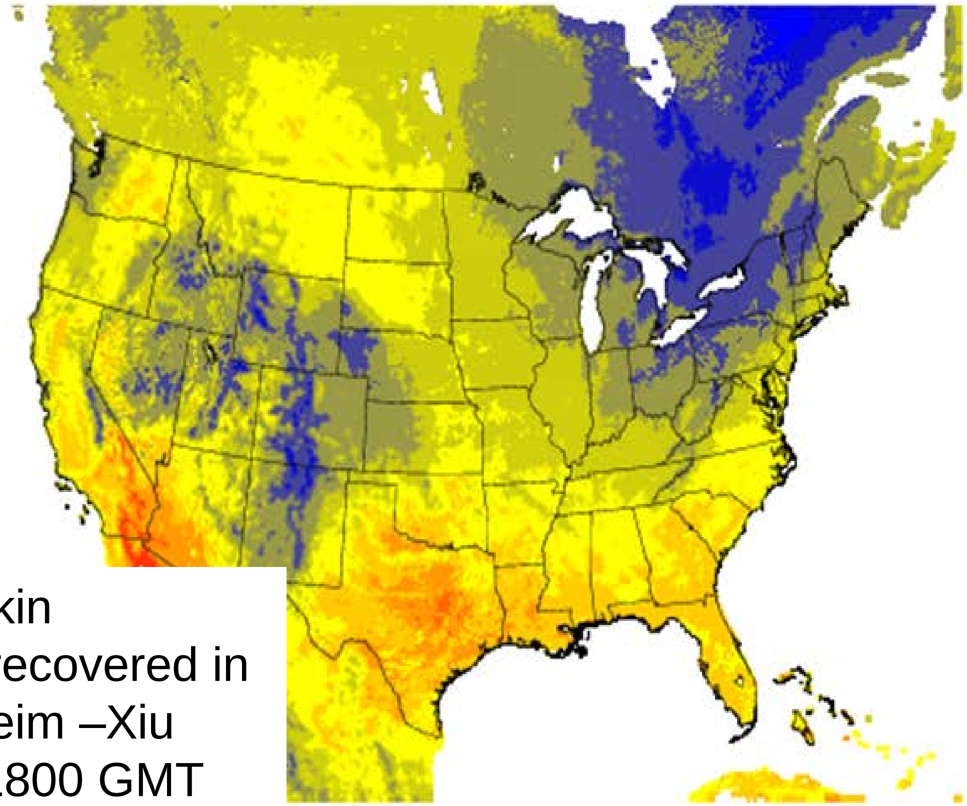

Example of skin temperature recovered in WRF from Pleim –Xiu scheme for 1800 GMT Sept 13, 2013

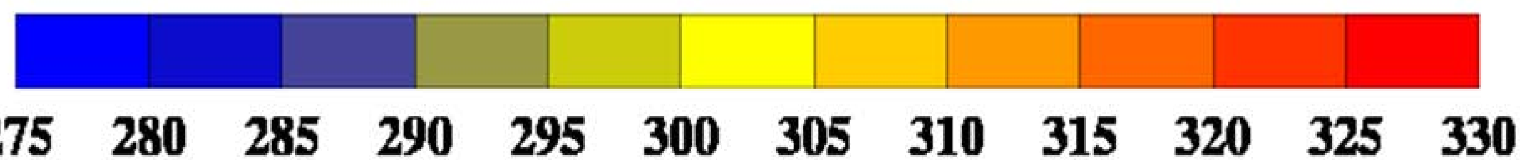

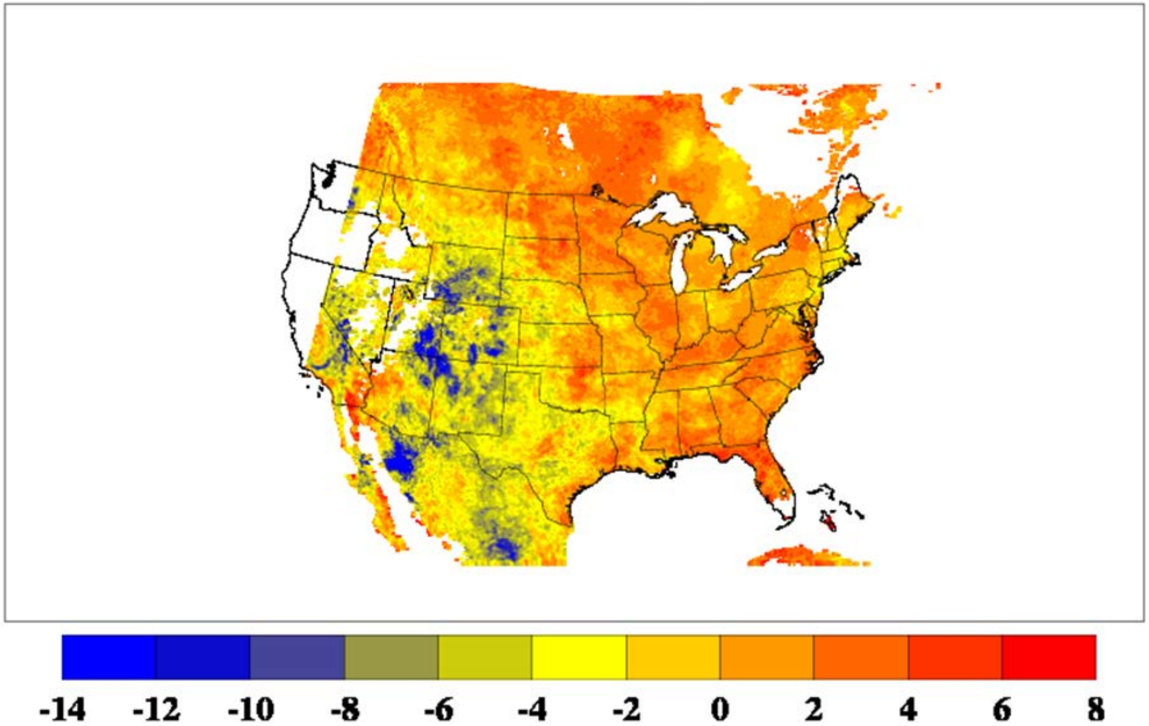

Fig. 6-4. Average daytime difference of the WRF diagnosed skin temperature minus the NOAA ALEXI observed skin temperature for the period 0000 UTC 1 September 2013 through 0000 UTC 6 September 2013. The NOAA ALEXI observed skin temperatures are the most recent version with aggressive cloud screening. Simulation is the insolation replacement run with the new (USGS) vegetation fraction and without any nudging. Values truncated between -14 and +8

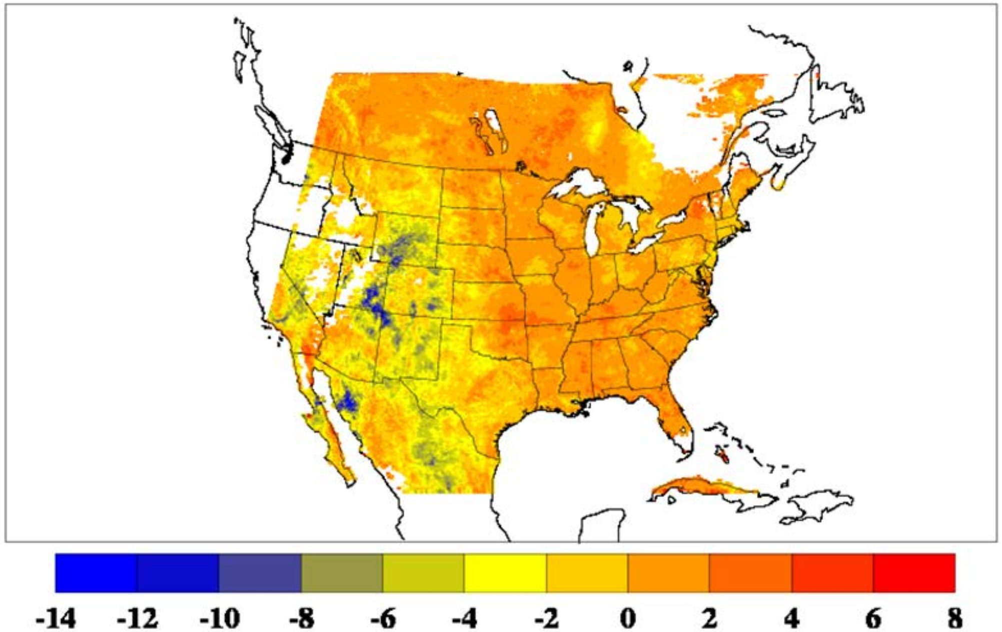

Fig. 6-5. Average daytime difference of the WRF diagnosed skin temperature minus the NOAA ALEXI observed skin temperature for the period 0000 UTC 1 September 2013 through 0000 UTC 6 September 2013. The NOAA ALEXI observed skin temperatures are the most recent version with aggressive cloud screening. Simulation is the insolation replacement run with the new (USGS) vegetation fraction with soil nudging (shallow and deep) with a nudging time scale of 600 s.

Potential of Skin Temperature to Improve WRF Performance

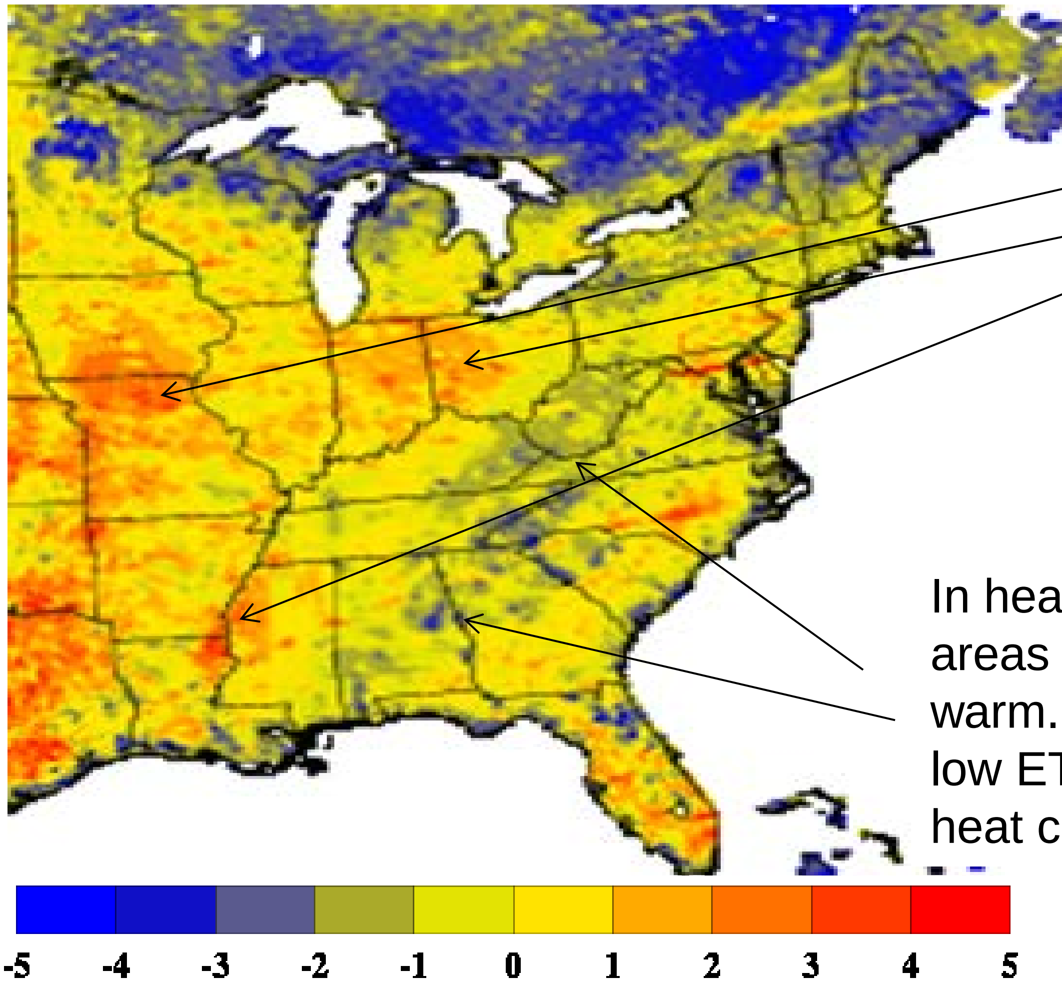

In September corn has been harvested and no longer transpiring. WRF is cooler than satellite likely has too much ET or too large heat capacity

In heavily forested areas WRF is too warm. May have too low ET or too small heat capacity

Difference between GOES Skin Temperature and WRF Control

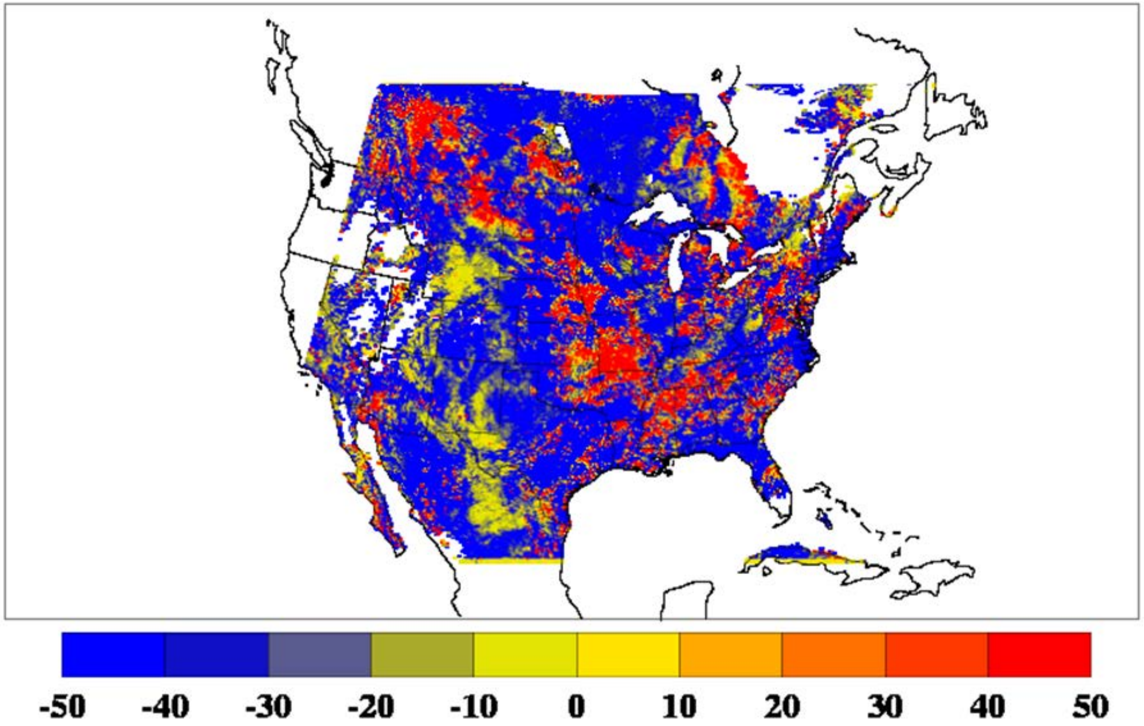

Fig. 6-6. Percentage change of the magnitude of the soil nudging bias (BN, absolute value of bias) relative to the magnitude of the insolation bias (BI, absolute value of bias) as given by 100 (BN – BI) / BI. This is the P statistic given by equation (7). Values truncated to ± 50 %. Both simulations used the USGS vegetation fraction. The NOAA ALEXI observed skin temperatures are the most recent version with aggressive cloud screening. Both simulations are for the period 0000 UTC 1 September 2013 through 0000 UTC 6 September 2013. Bias values are daytime only.

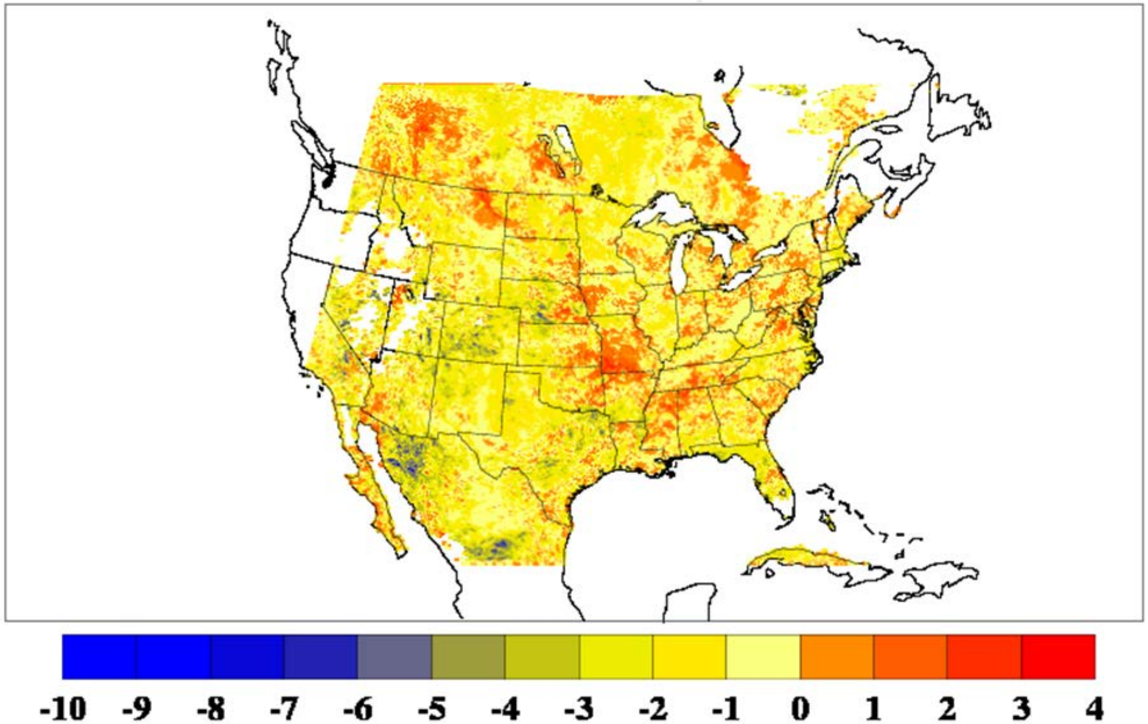

Fig. 6-7 Difference between the magnitude of the soil nudging bias (BN, absolute value of bias) and the magnitude of the insolation bias (BI, absolute value of bias) as given by BN – BI in units of K. This is an unscaled version of the P statistic given in (7) - i.e. without the division of by $B_{I.}$ The NOAA ALEXI observed skin temperatures are the most recent version with aggressive cloud screening. Both simulations are for the period 0000 UTC 1 September 2013 through 0000 UTC 6 September 2013. Bias values are daytime only. Same information as in Fig. 6.6 but not normalized with respect to the insolation bias. Negative values (cool colors) correspond to a reduction in the magnitude of the bias, and positive values (warm colors) correspond to an increase in bias

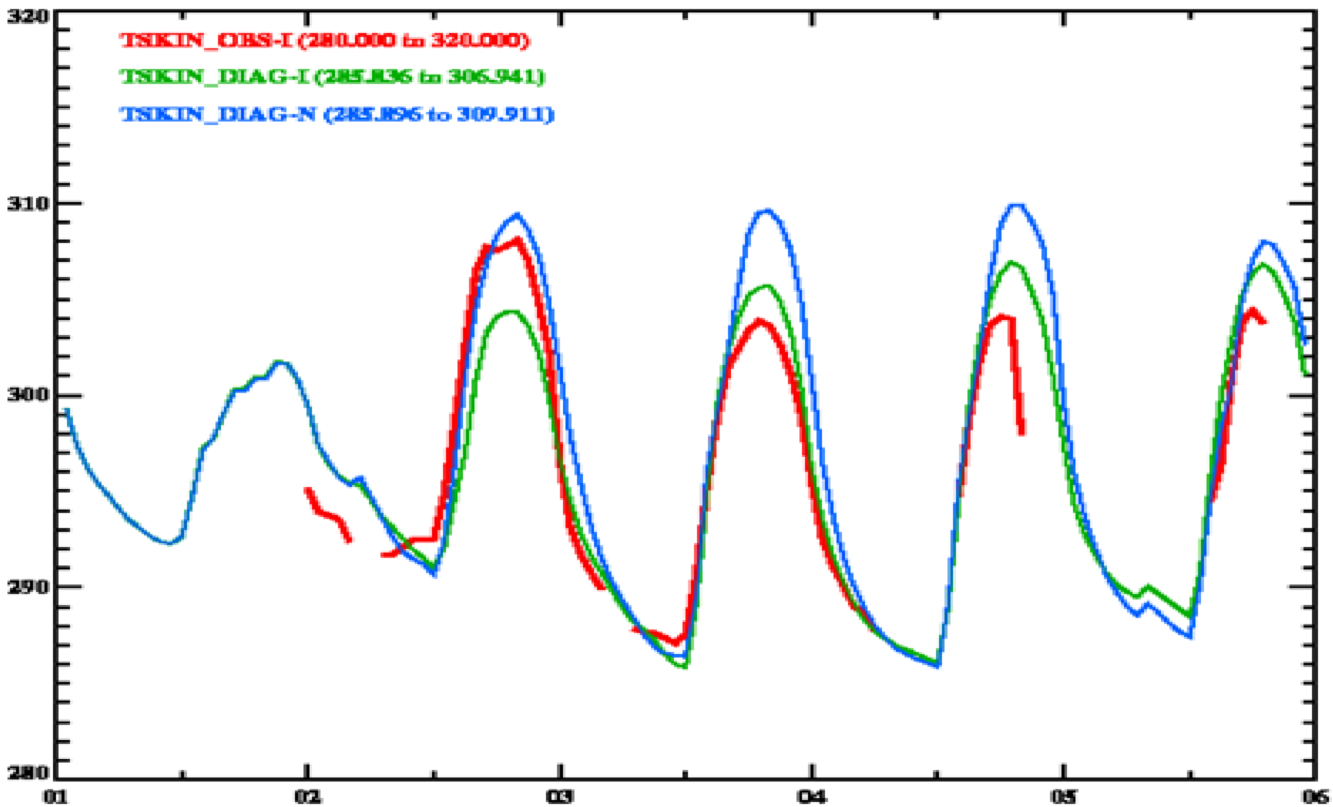

Fig. 6-9. Time series for 0000 UTC 1 September 2013 through 0000 UTC 6 September 2013 for southwestern Missouri (location code "A") This is a location where the magnitude of the bias increased with soil nudging.

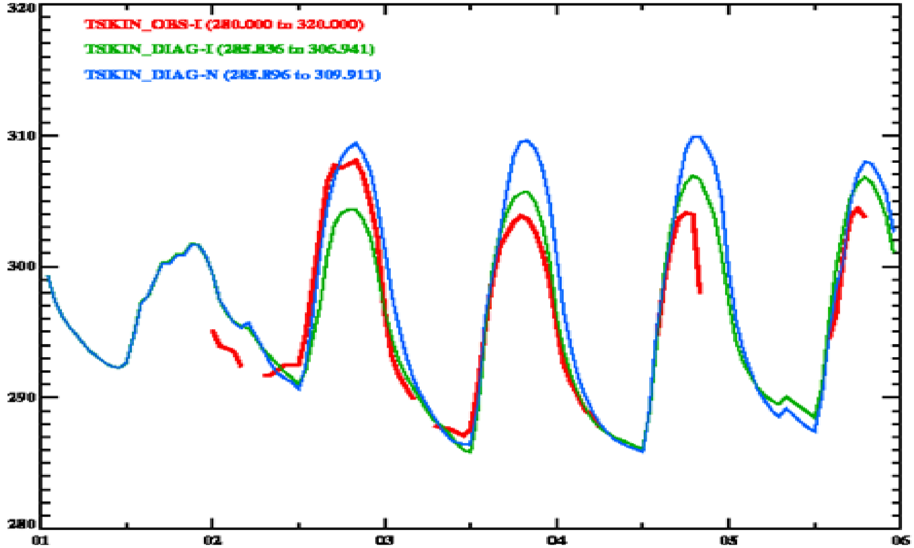

Corrects on second day by reducing moisture. But following days increases error

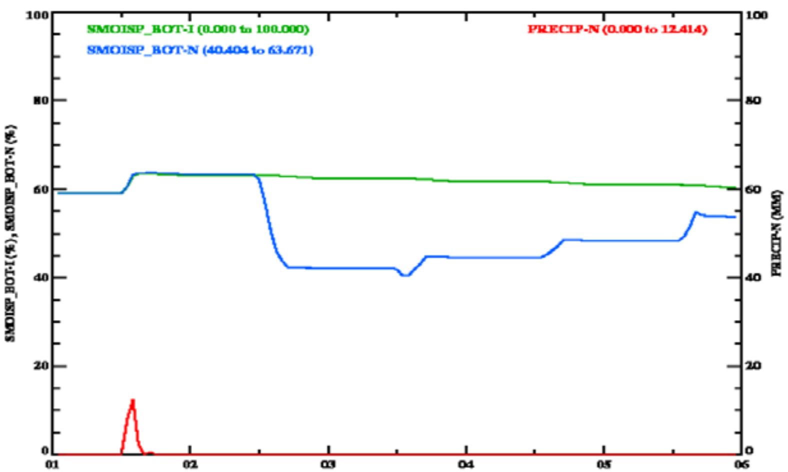

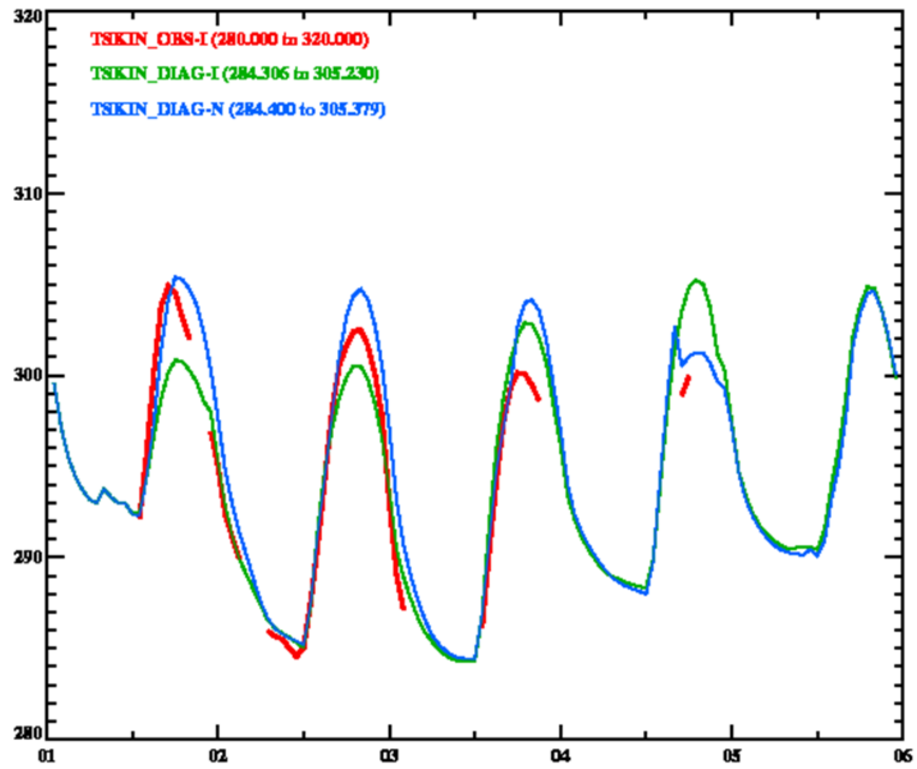

Fig. 6-11. Time series for 0000 UTC 1 September 2013 through 0000 UTC 6 September 2013 for western Iowa (location code "B") This is a location where the magnitude of the bias increased with soil nudging.

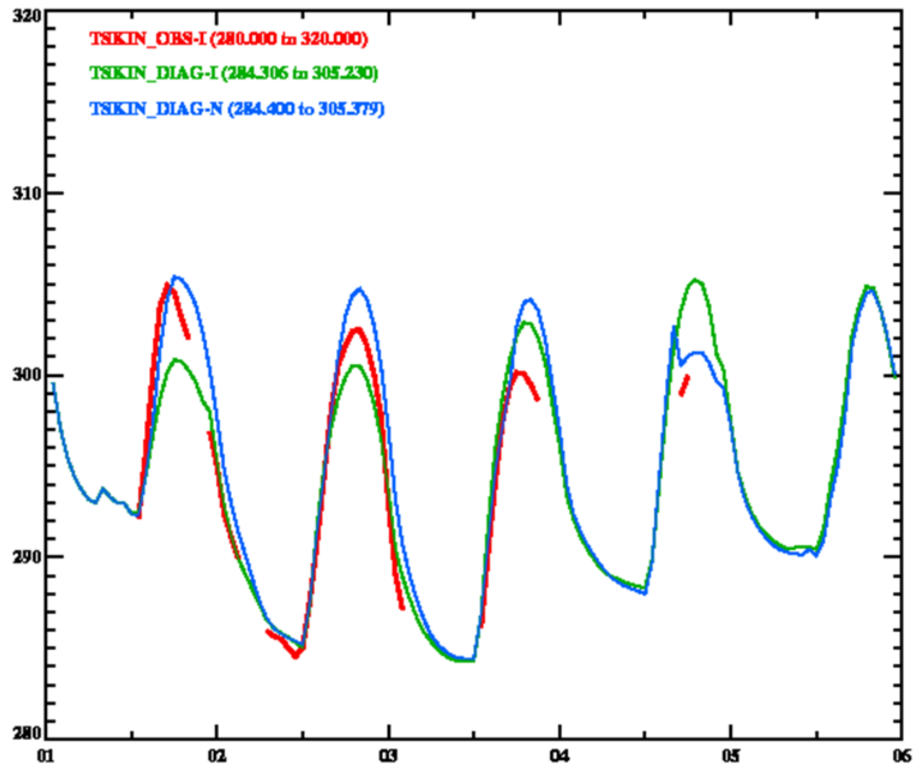
TSKIN_OBS-I (280.000 to 320.000)
TSKIN_DIAG-I (284.306 to 305.230)
TSKIN_DIAG-N (284.400 to 305.379)
320
310
300
290
280
01
02
03
04
05
06

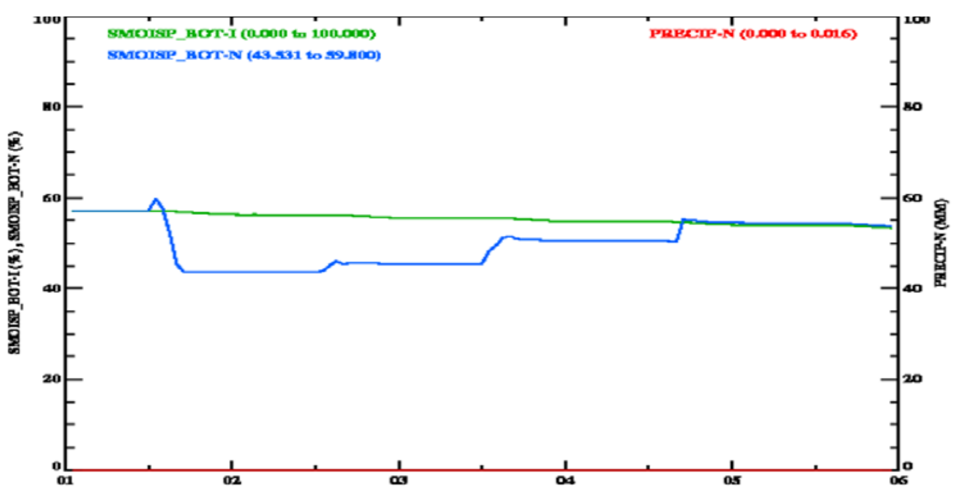
SMOISP_BOT-I (0.000 to 100.000)
SMOISP_BOT-N (43.531 to 59.800)
PRECIP-N (0.000 to 0.016)
SMOISP_BOT-I (%), SMOISP_BOT-N (%)
PRECIP-N (MM)
100
80
60
40
20
0
01
02
03
04
05
06

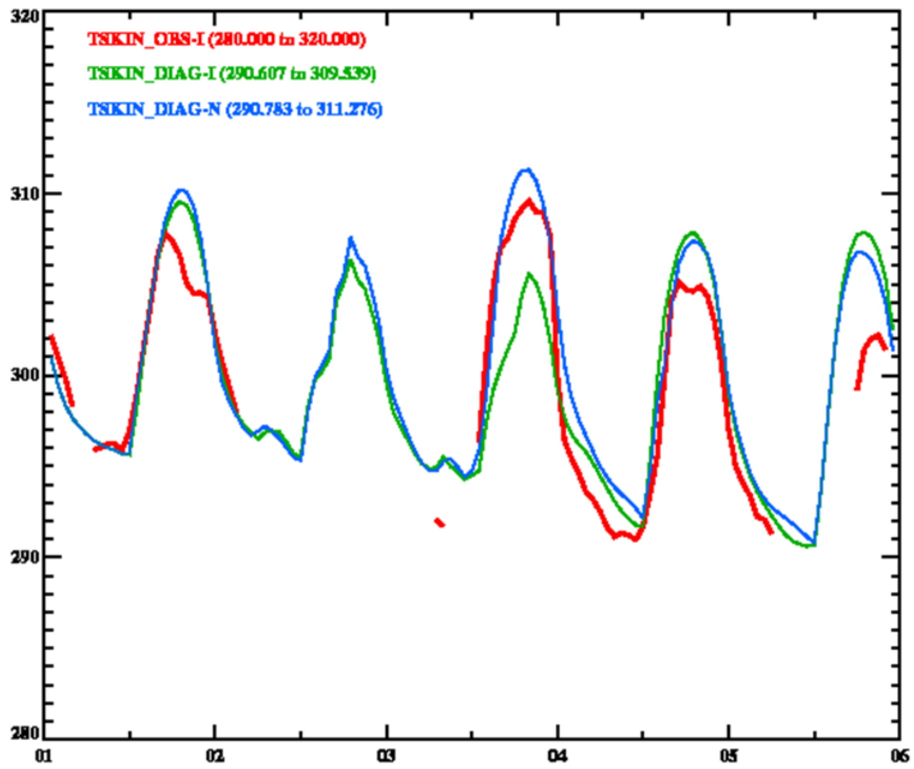

Fig. 6-13. Time series for 0000 UTC 1 September 2013 through 0000 UTC 6 September 2013 for northwestern Alabama (location code "C") This is a location where the magnitude of the bias increased with soil nudging.

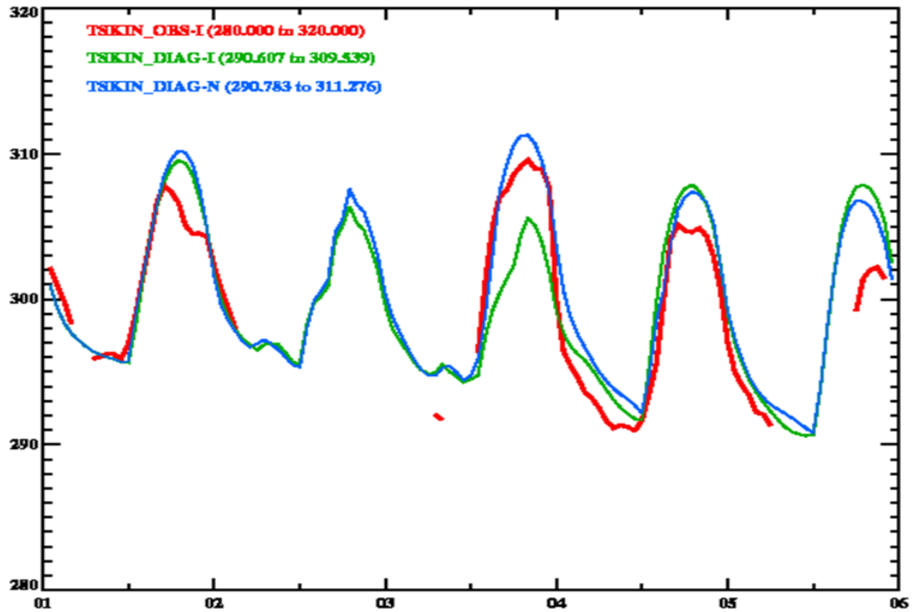

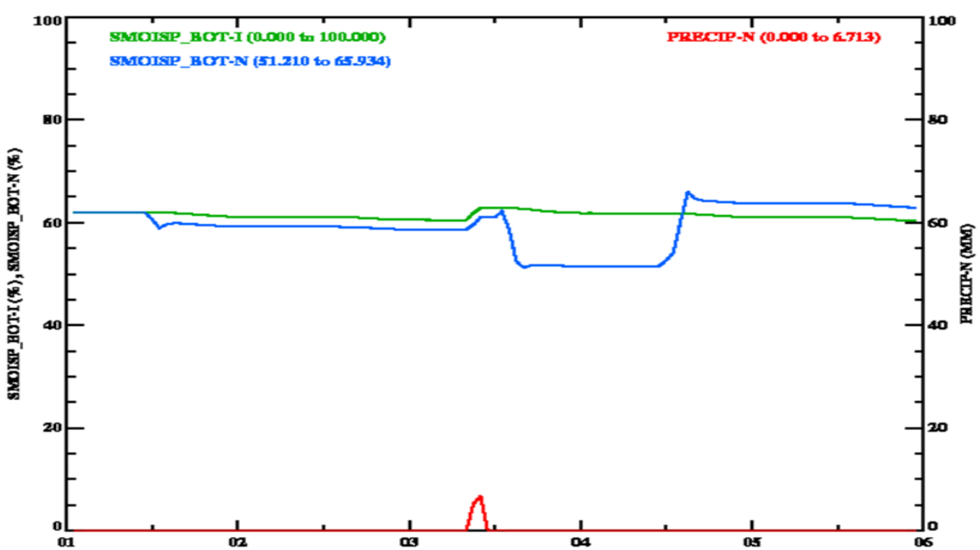

Bay Area Air Quality Management District
California Resources Board
Georgia
TCEQ
NASA
NOAA
NSSTC
RICE
The University of Alabama in Huntsville

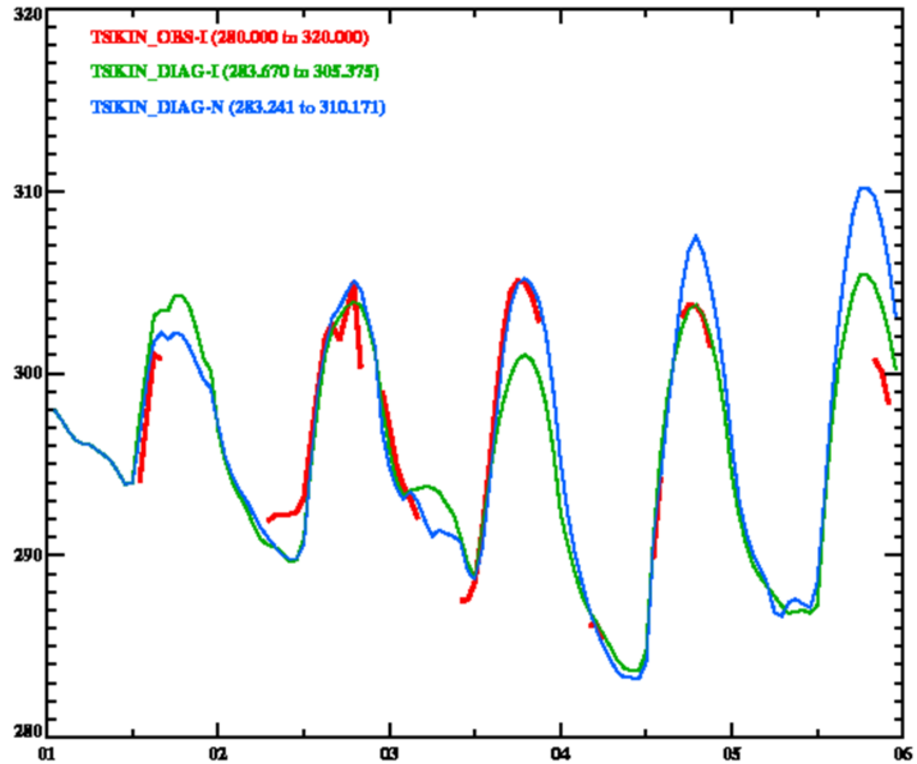

Fig. 6-15. Time series for 0000 UTC 1 September 2013 through 0000 UTC 6 September 2013 for southern Indiana (location code “D”) This is a location where the magnitude of the bias increased with soil nudging.

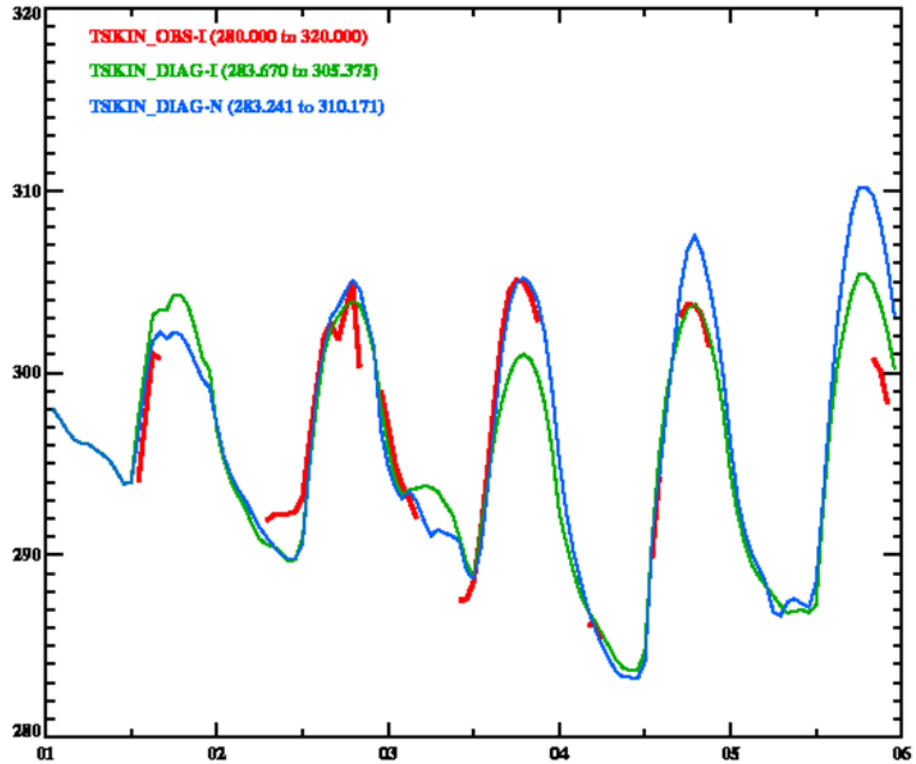

TSKIN_OBS-I (280.000 to 320.000)
TSKIN_DIAG-I (283.670 to 305.375)
TSKIN_DIAG-N (283.241 to 310.171)
320
310
300
290
280
01
02
03
04
05
06

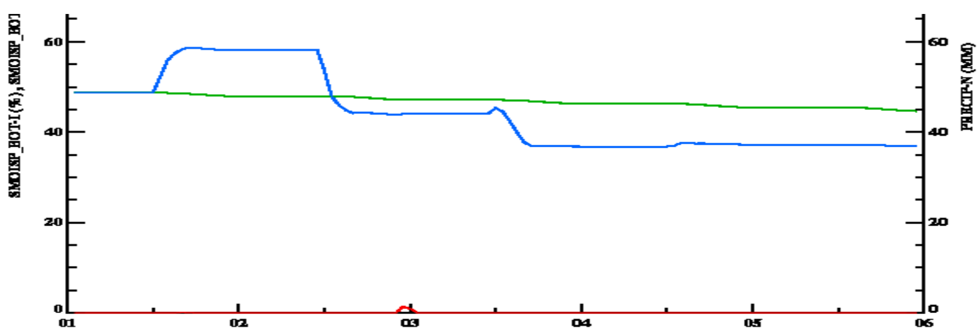

SMOISP_BOT-I (%), SMOISP_BOT
PRECIP-N (MM)
60
40
20
0
01
02
03
04
05
06

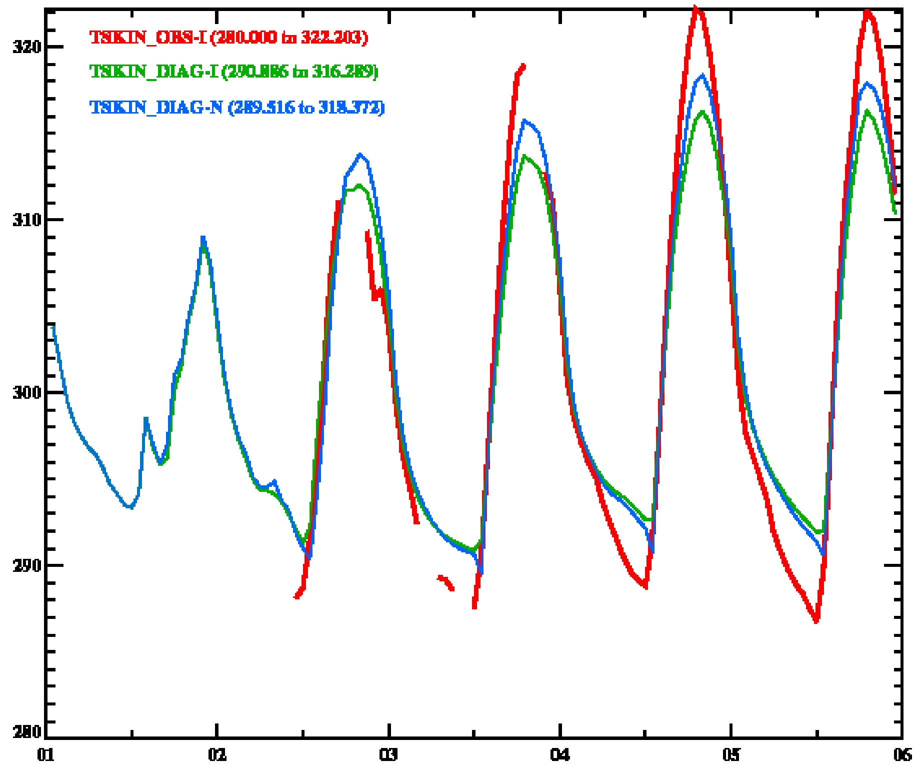

Fig. 6-17. Time series for 0000 UTC 1 September 2013 through 0000 UTC 6 September 2013 for northern Texas (location code "EThis is a location where the magnitude of the bias decreased with soil nudging.

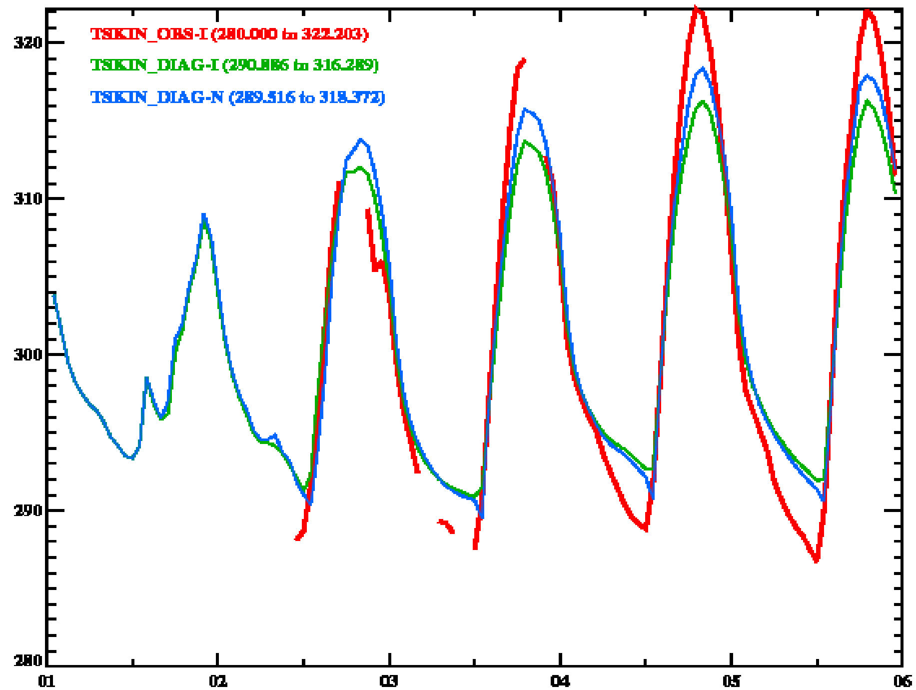
TSKIN_OBS-I (280.000 to 322.203)
TSKIN_DIAG-I (290.886 to 316.289)
TSKIN_DIAG-N (289.516 to 318.372)
320
310
300
290
280
01
02
03
04
05
06

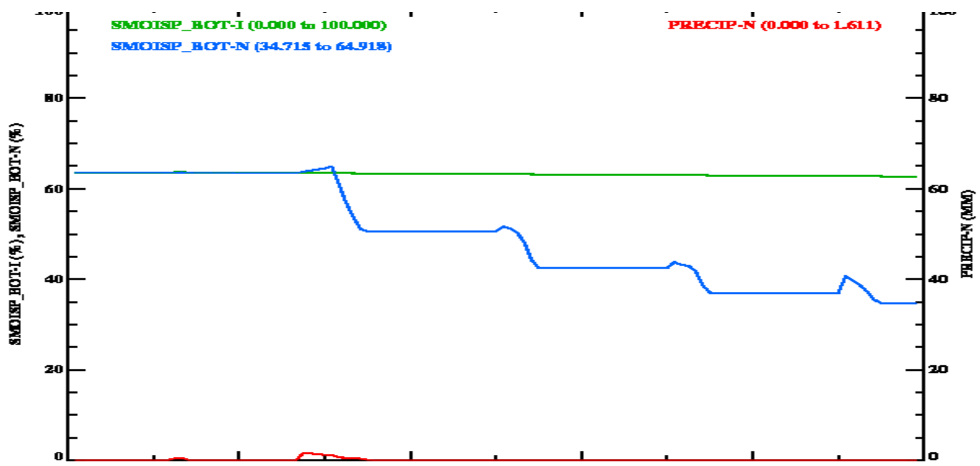
SMOISP_BOT-I (0.000 to 100.000)
SMOISP_BOT-N (34.715 to 64.918)
PRECIP-N (0.000 to 1.611)
SMOISP_BOT-I (%), SMOISP_BOT-N (%)
PRECIP-N (MM)
80
60
40
20
0
01
02
03
04
05
06